Intermittency and the Value of Renewable Energy

Gautam Gowrisankaran

University of Arizona, HEC Montreal, and National Bureau of Economic Research

Stanley S. Reynolds

University of Arizona

Mario Samano

HEC Montreal

A key problem with solar energy is intermittency: solar generators produce only when the sun is shining, adding to social costs and requiring electricity system operators to reoptimize key decisions. We develop a method to quantify the economic value of large-scale renewable energy. We estimate the model for southeastern Arizona. Not accounting for offset carbon dioxide, we find social costs of $138.40 per megawatt hour for 20 percent solar generation, of which unforecastable intermittency accounts for $6.10 and intermittency overall for $46.00. With solar installation costs of $1.52 per watt and carbon dioxide social costs of $39.00 per ton, 20 percent solar would be welfare neutral.

We thank Rob Clark, Allan Collard-Wexler, Joseph Cullen, Lucas Davis, Meredith Fowlie, Ken Gillingham, Ben Handel, Bill Hogan, Paul Joskow, David Keith, Derek Lemoine, Ariel Pakes, Philipp Schmidt-Dengler, Juha Teirilä, Catherine Wolfram, John Wooders, Mo Xiao, Gregor Zoettl, the referees, editor, and seminar and conference participants at numerous institutions for helpful comments; Alex Cronin and the University of Arizona Photovoltaics Research Lab for providing solar PV data; and Valentina Kachanovskaya and Anatolii Kokoza for research assistance. We acknowledge research support from the Arizona Research Institute for Solar Energy. Data are provided as supplementary material online.

Electronically published June 29, 2016
[*Journal of Political Economy*, 2016, vol. 124, no. 4]

I. Introduction

> Like just about everyone who has looked at the numbers on renewable energy, solar power in particular, I was wowed by the progress. Something really good is in reach. (Paul Krugman, *New York Times*, April 21, 2014)

> For weeks now, the 1.1 million solar power systems in Germany have generated almost no electricity. . . . As is so often the case in winter, all solar panels more or less stopped generating electricity at the same time. To avert power shortages, Germany currently has to import large amounts of electricity [including by] powering up an old oil-fired plant in the Austrian city of Graz. (*Der Spiegel*, January 16, 2012)

Across the world, renewable energy capacity has increased dramatically as a result of falling prices, policies favoring renewable energy, and concern over greenhouse gas emissions from fossil fuel generators. A key problem with generation from solar and other renewable sources is intermittency: solar generators produce only when the sun is shining.[1] Intermittency has the potential to hugely affect the economic value, or equivalently the social costs, of renewable energy. The above *Der Spiegel* quote suggests that electricity system operators use costly backup generation to manage the intermittency of large-scale solar. More generally, the implementation of large-scale solar may require significant changes in key decisions of investment, operations, and demand-side management to mitigate its social costs.

This paper develops a method to quantify the social costs and reductions in carbon emissions from large-scale renewable energy generation. We estimate social costs by solving for the decisions that maximize total surplus under different levels of renewable energy capacity. Social costs depend crucially on (1) the variability of the source including the extent to which the variability correlates with demand, (2) the extent to which output from the source is forecastable, and (3) the costs of building backup generation required to maintain system reliability. We use our model to estimate the social costs of solar power for one grid area as well as to understand how the social costs vary under complementary policy environments such as greater real-time pricing. Our method can also be used to examine the social costs of different sources of renewable energy and in different contexts.

What does our economic analysis bring to the table? While there exists a systems engineering literature that evaluates the costs of renewable en-

[1] Notably, intermittency is a big issue for wind power as well, and wind is the largest source of renewable energy besides hydroelectric power (EIA 2012).

ergy, our welfare-maximizing economic analysis is fundamentally different. We reoptimize operator decisions as a function of renewable energy penetration, which requires balancing the consumer welfare lost from system outages and demand-side management against the extra costs of maintaining and using backup capacity. Without reoptimization, output fluctuations from large-scale solar will lead to suboptimal decisions—for example, overly high probabilities of system outage or excess investment in backup capacity—which add to social costs. Moreover, an economic model such as the one we develop is necessary to understand differences in social costs across complementary policy environments.

The starting point for our analysis is section 4 of Joskow and Tirole (2007), which models a system operator of an electricity market who seeks to maximize expected welfare when faced with fossil fuel generators that can suddenly fail. Our framework builds on Joskow and Tirole's by modeling renewable energy intermittency as similar to the unexpected failure of a traditional generator and by modeling a variety of factors (stochastic and variable demand, duration of system outages, generation and reserve costs for existing and new generators) that allow us to use available data in relatively simple ways. A contribution of our paper is to show how to take this theoretical model to data and use it to evaluate the social costs of renewable energy.

In our model, the system operator is faced with a fixed level of solar generation capacity as specified by an exogenous policy mandate. Initially, the operator chooses how many new fossil fuel generators to build and sets the price for contracts that curtail demand for flexible customers in periods of scarcity. Following this, in each (1-hour) period the operator is faced with a distribution of demand and, in the presence of renewables, a joint distribution of demand and renewable output. Observing the distribution, the operator must then decide how many generators to schedule for generation and reserves and how much demand to curtail. Finally, demand and solar output are realized, resulting in a system outage if generation and reserves are insufficient to meet demand.

We apply our model to the Tucson, Arizona, grid area. We obtained solar output data from 58 geographically dispersed sites in the Tucson area. We complement these data with a variety of cost and failure information on generators, day-ahead weather forecast data, and demand information. We forecast the demand and renewable output distributions that are observable to the operator with regressions of demand and renewable outputs on the weather forecasts made the previous day. We calibrate the demand elasticity from the literature.[2]

[2] Alternatively, we could structurally estimate demand by matching operating reserves from data to predicted values assuming optimizing behavior. However, we believe that it may be problematic to assume that current Tucson Electric Power (TEP) decisions reflect

It is well understood that the average accounting cost of solar is higher than for fossil fuel generators. Not surprisingly, we find that the gross social costs of solar are high and increasing in penetration, going from $126.70 per megawatt hour (MWh) with 10 percent penetration to $138.40 per MWh with 20 percent penetration. The increase in cost from increased solar penetration is caused by solar generation substituting for cheaper fossil fuel plants as penetration rises. Dividing the social costs by the carbon dioxide (CO_2) reductions, a ton of CO_2 would have to have an environmental cost of $275 or more to justify immediate large-scale investment in solar, a figure that is much higher than the 2015 central US government figure of $39 (EPA 2015).

Perhaps more surprising than the high cost is a breakdown of its sources. Focusing on the 20 percent case, if solar were perfectly forecastable, the social costs would drop very little, by $6.10 per MWh. With perfect storage of solar, social costs would drop by $46 per MWh, implying that intermittency overall is quantitatively much more important than unforecastable intermittency. In contrast, the bulk of the cost of solar comes from its relatively high fixed costs: if the fixed costs of solar dropped from their current level of $4.41 per watt (W) to $2 per W (as is reflected by the Krugman quote and as many industry observers believe will occur), then the social cost of solar would drop by $99 per MWh.

We find that geographic dispersion of solar sites is important in lowering the social costs of solar generation: if all solar facilities were located within 10 kilometers of the center of Tucson, the social costs of 20 percent solar would rise by $17 per MWh relative to the base case of sites located within a 40-kilometer radius. In contrast, other changes to the environment—notably allowing imports and exports, having forecasts made less than 1 day ahead, and placing a substantial percentage of customers on real-time pricing contracts—have very limited impacts on the social costs of solar.

Our work builds on both a systems engineering and economics literature on valuing renewable energy. One strand of the systems engineering literature focuses on the variability of renewable output and allows for changes in utility operations to be based on rules of thumb, rather than reoptimizing policies in response to the renewable energy (see, e.g., Fabbri et al. 2005; Mills and Wiser 2010; Lueken, Cohen, and Apt 2012). A second strand uses optimization models from power systems engineering (see, e.g., GE Energy 2008; Tuohy et al. 2009; Madaeni and

optimizing behavior within the context of our model. For instance, Wolfram (2005) finds evidence that regulated investor-owned utilities (such as TEP) operate generation units at higher cost than do nonregulated utilities. Furthermore, the TEP system operator may act in a more risk-averse manner than in our model because of both career concerns and regulatory penalties for system outage.

Sioshansi 2013; Mills et al. 2013). The analyses in these papers specify the cost-minimizing combinations of generation units necessary to meet forecasted demand and operating reserve requirements.[3] However, this strand limits optimization to the generator scheduling decision, with changes to reserve operations and fossil fuel capacity still based on rules of thumb. We find that a system operator who followed rules of thumb from this literature would face social costs that are significantly higher than with optimizing policies.

An economics literature also seeks to quantify the importance of intermittency.[4] One strand of this literature focuses on how the time-varying generation profile of renewable energy affects its value (see Denholm and Margolis 2007; Borenstein 2008; Cullen 2010b; Joskow 2011). A natural starting point of valuation for some of these papers is the equilibrium price of renewables, but since prices are informative only for valuations at the margin, a price-based approach cannot easily be used to evaluate policies that lead to large-scale investment in renewables. A second strand addresses how fossil fuel capacity should be adjusted in response to large-scale renewables but often does not focus on the time-varying generation profile of renewable energy (see Lamont 2008; Skea et al. 2008; Campbell 2011).[5] Our model combines insights from both these strands. To our knowledge, our study is the first to formalize reserve operations in an economic model that is taken to data and the first to use weather forecast data to separate intermittency into its forecastable and unforecastable components.

The remainder of the paper is organized as follows. Section II provides background on the electricity market and solar energy. Section III discusses the model; Section IV the data, estimation, and computation; and Section V the results. Section VI presents conclusions.

II. Electricity and Solar Energy

A. *The Electricity Industry in the Tucson Area*

We now discuss some details of our market and explain how they motivate our later modeling assumptions. We model the Tucson grid area, which includes most of southeastern Arizona. Electricity service is provided by Tucson Electric Power (TEP), a vertically integrated, investor-owned regulated utility. TEP's service territory covers 1,155 square miles

[3] An advantage of this strand over our paper is that it often models dynamic linkages (e.g., ramping constraints and start-up costs) within a day. Our base model does not allow for dynamics, but we provide robustness analysis that quantifies the additional generator start-up costs from large-scale solar.

[4] See Baker et al. (2013) for a review of this literature.

[5] In an exception, Lamont (2008) does include time-varying generation.

and includes a population of approximately 1 million.[6] In 2011, 41 percent of TEP retail electricity consumption was residential, 21 percent commercial, and 38 percent industrial and public. During this time period, average retail prices were 9.9 cents/kWh for residential customers and 9.4 cents/kWh for commercial and industrial customers (UniSource 2012). Our simulations specify a fixed retail price that lies between these two values.

As of the end of 2011, TEP owned or leased generation units with a total capacity of 2,275 megawatts (MW). This capacity is virtually all powered by fossil fuel. In Arizona, there are 2,090 MW of planned new fossil fuel generation capacity, all of which are from natural gas generators. Combined cycle natural gas generators have lower marginal costs and greenhouse gas emissions but higher construction costs than other natural gas generators. Ninety-one percent of the planned new fossil fuel capacity in Arizona is from combined cycle generators, with the remaining from gas turbine generators. Nationally, 88 percent of planned new natural gas capacity is combined cycle.[7] Given these figures, our base specifications allow new fossil fuel investment only in combined cycle natural gas generators.

Tucson is situated within the Western Interconnection, the electrical grid that encompasses the western United States and part of western Canada. TEP is responsible for system operations and for scheduling generation and transmission power flows within its grid area. At different times, TEP both imports and exports power over the Western Interconnection. Our base model treats Tucson in isolation, but we also consider robustness specifications that allow for imports and exports.

TEP is subject to a state-mandated Renewable Portfolio Standard, which calls for an increasing fraction of load to be generated from renewable sources until 15 percent of load is from renewables by 2025. For 2011 the standard was 3 percent. TEP satisfies the standard through a combination of its own solar generation, wholesale purchases of renewable energy, distributed solar generation by its customers, and retirement of banked renewable energy credits.[8] Total distributed (i.e., customer-sited) solar capacity in TEP's service territory was 30.4 MW as of the end of 2011, enough to supply 0.3 percent of annual electricity consumption (TEP 2012, table 2.1). Given its small scale and lack of available data, we do not model the distributed solar that is already present in our base environment. The Renewable Portfolio Standard figure of 15 percent, together with the near absence of wind generation in Ari-

[6] Detailed information about TEP customers and operations are found in the 2011 10-K annual report for UniSource Energy Corp., TEP's parent company (see UniSource 2012).

[7] Source: Authors' calculations from EIA (2014a, table 6.5).

[8] TEP owns no wind generation. While there is some wind generation in Arizona, wind is not expected to be a major source of renewable generation in the state.

zona, motivates our choice of examining scenarios in which 10, 15, and 20 percent of generation is from solar.

Since storage is very limited for TEP and most electricity systems, the supply of power must equal (almost exactly) load on a real-time basis. Moreover, load can vary unpredictably over the course of a day (e.g., because of weather changes), and available supply can vary quickly and unpredictably because of equipment malfunction or breakdown and because of intermittent renewable generation. To ensure matching of supply and load, the electricity grid operator engages in *system operations*. System operations involve control of generators, decisions about rationing power to customers, and control of backup systems. The system operator ensures reliability in part by having generators available on a standby basis so that customers can continue to be served in the event that one or more generators fail and/or load exceeds forecast. In the absence of grid operations, each supplier imposes externalities, because it does not bear the full cost of a system outage (see Joskow and Tirole 2007). The modeling of system operations, and endogenizing system operations in response to large-scale solar, is a key part of our analysis.

The generation capacity that is scheduled by the system operator over and above the amount required to serve forecasted load is called *operating reserves*. Broadly speaking, utilities carry two types of operating reserves: contingency reserves, used in the event of a generator failure, and balancing reserves, used to smooth out fluctuations in load and renewable output. The North American Electric Reliability Corporation (NERC) requires utilities in the Western Interconnection to have access to contingency reserves sufficient to cover the failure of their largest unit (see NERC 2015); for TEP this is a 403 MW coal generator, which is 20.9 percent of mean load. Ela, Milligan, and Kirby (2011) note that balancing reserves are typically set between 1 and 1.5 percent of peak load. Together, these imply that TEP should maintain approximately a 23 percent ratio of operating reserves to load.[9] The 23 percent ratio provides a benchmark against which we can compare the baseline predictions of our model.

B. Solar Energy

Solar photovoltaic (PV) systems utilize panels of materials (typically silicon) that convert solar radiation into direct current (DC) electricity, coupled with inverters that convert DC to alternating current (AC)

[9] Operating reserves may be lower because TEP is part of the Southwest Reserve Sharing Group. Participation in this group allows TEP to call on other utilities during emergencies, such as plant outages and system disturbances, and reduce the amount of reserves TEP is required to carry (UniSource 2012).

(see National Renewable Energy Laboratory 2011). Electricity generation from solar PV panels varies with solar insolation, a measure of energy from sunlight. Solar PV technology has been improving rapidly.[10]

Investment in solar PV capacity has grown considerably in recent years, while wind capacity investment has recently declined. Roca (2013) projects that solar PV capacity investment would exceed wind capacity investment worldwide in 2013. Figure 1 shows solar insolation across the United States. The Tucson area has a relatively high solar insolation as does most of the Southwest, which constitutes about one-fifth of the continental US land mass.

Because open land is plentiful near population centers in the southwestern United States, it is common to locate large utility-scale solar PV near existing transmission links. New plants have to pay and report *interconnection costs*, which cover the extra transmission costs necessary to tie them into the grid. In Arizona, the mean interconnection costs for plants built between 2003 and 2011 were $45,454 per MW for natural gas combined cycle plants and $64,802 for solar PV plants (EIA Form 860, http://www.eia.gov/electricity/data/eia860/). Applying our data on solar production rates and our assumed discount factor and plant lifespan to these numbers, the extra interconnection costs for solar are very small, about $0.78 per MWh generated, and hence we do not model these extra costs.

In addition, Arizona's Renewable Portfolio Standard mandates that 30 percent of total renewable energy consist of distributed generation, for example, solar PV on customers' rooftops. Our model allows distributed solar to have different capital costs from nondistributed solar and to reduce electricity transmission costs.

To illustrate the issues of intermittency, figure 2 shows load and solar PV output for four sites across the United States, for three summer days during our sample period, August 14–16, 2011. We chose three sites from the western United States with high solar potential (fig. 1) as well as New York. During these three days, the solar installation in New York produces far below its rated capacity at all times. The other installations all reach a peak output of 75 percent of capacity or higher at some point each day and have similar normalized total output. None of the installations produce electricity at night, and output is minimal in the early morning and late evening.

For all four locations, the timing of load and solar production peaks is similar, which generates a positive correlation between load and solar output. The positive correlation increases the value of solar installations

[10] Baker et al. (2013) describe the variety of solar PV technologies that are currently available, as well as potential technological improvements that are likely to change PV cost and efficiency in the coming decades.

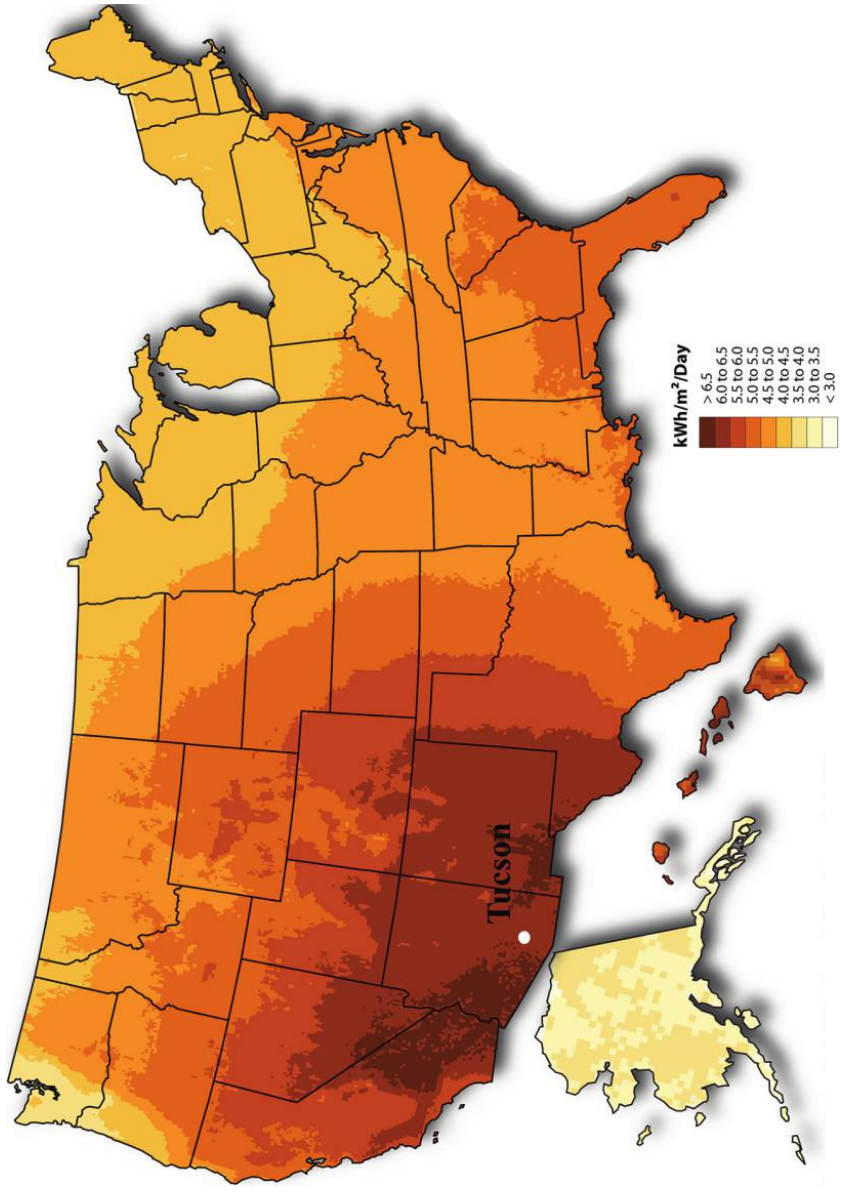

FIG. 1.—Photovoltaic solar resource. Source: National Renewable Energy Laboratory.

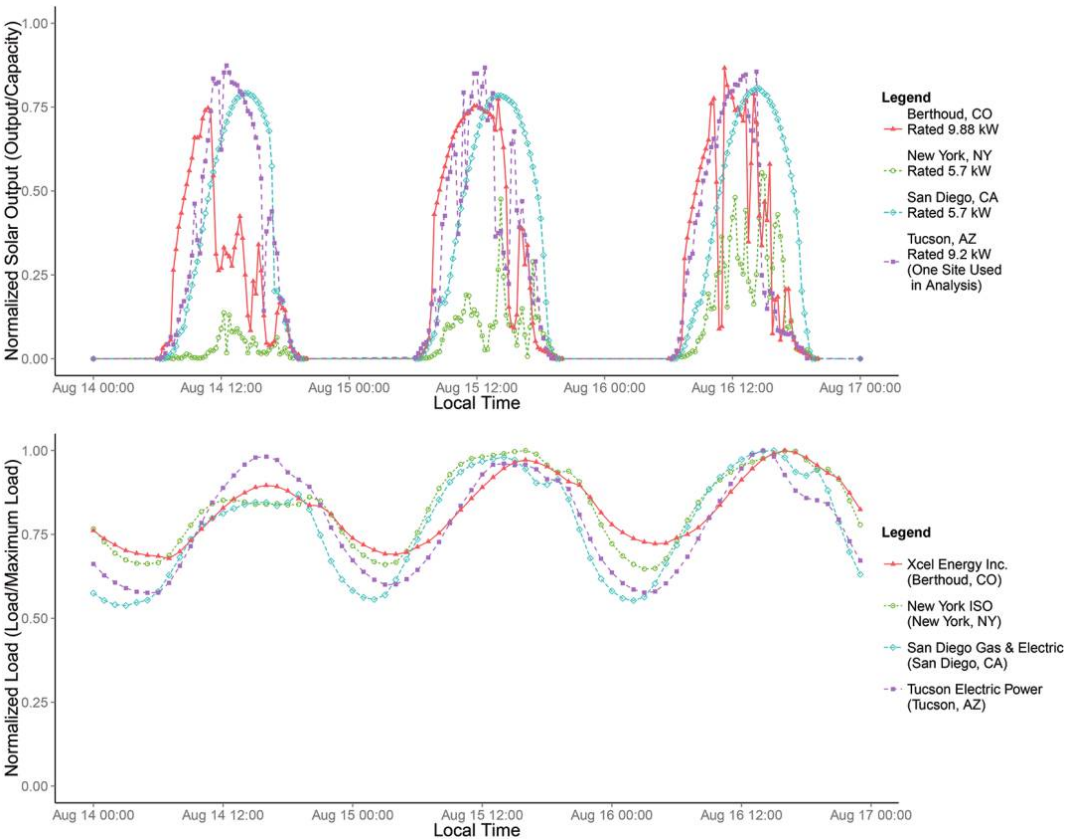

FIG. 2.—Load and solar output for different US sites, August 14–16, 2011. The Berthoud, New York, and San Diego solar generation data are from SMA Solar Technology AG's Sunny Portal (https://www.sunnyportal.com/). The Tucson data displayed here are from one of 58 sites used in our main analysis and are from the University of Arizona Photovoltaics Lab. The site shown here was chosen because it is near the center of the city. The load data are from FERC Form 714. Load is measured hourly while solar output is measured at the 15-minute level.

because production occurs when load and, hence, the marginal cost of displaced fossil fuel generation are high. Even though solar output correlates positively with load, peak load tends to occur later in the day than peak solar output. To the extent that system operators have to deal with late afternoons with high load but low solar output, they will not be able to reduce fossil fuel capacity much in the presence of large-scale solar.

Finally, note that during these three days, all the solar installations except for the San Diego facility show large fluctuations over a fine time scale. These fluctuations are not easily forecastable and hence will lead to increased reserve operation costs. Hence, ideally, solar output would look like the San Diego installation over these days rather than the others.

III. Model

A. *Overview*

We now describe our base model of electricity generation, demand, and system operations. Our model takes as given the retail price of electricity and a state-mandated level of solar capacity.

Our model has two stages. In stage 1, the system operator decides on capacity investment for new generation units, which are all combined cycle natural gas generators. The new generation units, solar capacity, and existing fossil fuel generators all last a fixed number of years. At this stage, the operator also chooses a price for interruptible power contracts and offers these contracts to customers.

In stage 2, the operator is faced with a sequence of generator scheduling and demand-side management decisions for each hour of each year over the life span of the generators.[11] Here, she observes the weather forecast (made the previous day) and a list of which fossil fuel generators will be unavailable because of scheduled maintenance. Observing this information, the operator forecasts load and solar output and then chooses which fossil fuel generators to schedule for production and reserves and how much load to curtail from the set of customers who have signed up for interruptible power contracts.[12]

In each hour, following the scheduling and curtailment decisions, solar output and load are realized and some fossil fuel generators may fail. These realizations lead to one of two possible outcomes. First, load could be less than the sum of electricity output and operating reserves, adjust-

[11] Our base model abstracts from linkages between hours, as would occur with ramping or start-up costs.

[12] System operators commonly schedule operating reserves 1 day ahead. For example, the system operator for the Electric Reliability Council of Texas (ERCOT) obtains operating reserves for each hour in 1-day-ahead procurement auctions.

ing for line losses. In this case, the operator will adjust the rate of generation for one or more generators to balance output with load. Second, load could be more than output plus reserves, adjusting for line losses. In this (it is hoped rare) case, a system outage occurs and a random subset of customers involuntarily lose power.

Appendix B includes extensions to this model in the form of multiple solar observations per hour, real-time pricing contracts, and imports and exports outside the market. We now exposit demand, generation, and the operator's solution.

B. *Demand and Consumer Welfare*

We assume that retail price is a constant $\overline{p}$. We need to specify the demand curve in order to quantify the costs of system outage and the take-up of interruptible power contracts. We let demand be a random function of the weather forecast, denoted $\vec{w}$. We let $\vec{w}$ include cloud cover, temperature, and similar variables as well as any factors that might affect load or solar output, notably the time of day, day of week, and time since sunrise and sunset.

We choose a parsimonious specification for demand in order to more easily calibrate the model. Specifically, we assume that demand has a constant price elasticity η for prices up to a reservation value, v, but that the scale $\overline{D}$ varies stochastically with $\vec{w}$, $\overline{D} \sim F^D(\cdot|\vec{w})$. Demand is then

$$Q^D(p, \overline{D}) = \begin{cases} 0 & p > v \\ \overline{D}p^{-\eta} & p \leq v. \end{cases} \tag{1}$$

We assume that $F^D(\cdot|\vec{w})$ has a lower bound $\overline{D}^{\min}(\vec{w})$.

The term *value of lost load* (VOLL) is used in the electricity industry to describe the mean value of electricity per unit for customers (see Cramton and Lien 2000). VOLL and the reservation value v have a closed-form and monotonic relation, detailed in Appendix A.

In our base model, the system operator manages demand through voluntary arrangements to curtail demand when necessary, in exchange for a payment at the time of curtailment. These contracts are known as pay-as-you-go interruptible power contracts (see Baldick, Kolos, and Tompaidis 2006). Many utilities offer this type of contract (see FERC 2012), and there exist firms (e.g., EnerNoc.com) that intermediate these contracts between small- to medium-sized commercial customers and utilities.

The specifics of our curtailment contracts are as follows. In the first stage, the operator offers interruptible power contracts at price p_c. Customers who sign up agree to have their power curtailed as necessary and be paid a net per-unit price of $p_c - \overline{p}$ as compensation. In each stage 2 pe-

riod, the operator chooses a quantity z of demand curtailment and randomly selects customers for curtailment from the set of customers who have signed up and who are known to use power in that period.[13]

The amount by which the system operator can curtail demand in any period is limited by the curtailment price p_c, as users will sign up for the interruptible contract if and only if their valuation is below p_c. Note that there is a trade-off from increasing p_c. An increase in p_c implies that the operator can curtail more demand, which increases expected welfare as it lowers the probability of a system outage. However, an increase in p_c also implies an increase in the average valuation of the curtailed user, which decreases welfare. Let $\text{WLC}(z, p_c)$ denote the *welfare loss from curtailment* in any stage 2 period; Appendix A derives a closed-form expression for $\text{WLC}(z, p_c)$ and shows that it does not depend on $\overline{D}$.

C. *Generation, Transmission, and Reserves*

We index existing generators by $j = 1, \ldots, J$. For any given hour, each unit has a maintenance status $m_j \in \{0, 1\}$, with $m_j = 1$ implying that the unit is unavailable for production. We assume that maintenance occurs with probability P_j^{maint} and that its occurrence is independent and identically distributed (i.i.d.) across periods and generators. At each stage 2 period, the system operator schedules available units for production and reserves; let on_j denote a 0–1 scheduling indicator. Note that $m_j = 1$ implies that $on_j = 0$.

Each unit uses a particular generation technology, for example, coal-fired steam turbine or combined cycle natural gas, and has marginal costs (MC) c_j and capacity k_j. Generators are used for both production and operating reserves. For any generator, we assume that the MC of reserves is a fraction c^r of the cost of producing electricity for whatever fraction of capacity of the generator is under reserve.[14]

We specify that each generator has a probability P_j^{fail} of failure in any hour. Analogously to P_j^{maint}, we assume that failure occurrences are also i.i.d. Maximum output from generation unit j is then given by

[13] We assume that it is not possible for the operator to curtail demand selectively from the lowest-valuation users. If possible, this would result in more efficient rationing.

[14] Our model of the cost of reserves is a simplification of a much more complicated problem. In reality, there are several types of costs associated with maintaining operating reserves. Fossil fuel generation units typically have minimum and maximum generation rates and need to be operating at or above the minimum in order to provide operating reserve. Some high-cost generation units may be operating at their minimum so that they have excess capacity from which reserves can be provided; this implies that some lower-cost generation units may be operating below their maximum, which then implies an increase in production costs due to reserves. Also, it may be necessary to incur start-up costs for some of these higher-cost units. Finally, units that are providing operating reserves are not available for maintenance, implying that there may be deferred maintenance costs associated with operating reserves.

$$x_j(on_j) = \begin{cases} k_j & \text{with probability } (1 - P_j^{\text{fail}})on_j \\ 0 & \text{otherwise.} \end{cases} \tag{2}$$

Let $\overrightarrow{x}(\overrightarrow{on})$ denote the vector of maximum outputs for all generators.

Moving back to stage 1 of our model, the system operator chooses the number of new fossil fuel generators, n^{FF}. Each of the new units is an identical combined cycle gas generator, with the same failure and maintenance probabilities as existing gas generators. We assume that each has fixed capacity k^{FF}, capacity costs of FC^{FF} per MW of capacity, and operating costs of c^{FF} per MWh. We label the new fossil fuel units $j = J + 1, \ldots, J + n^{FF}$.

The system operator is faced with a fixed solar PV capacity n^{SL}, which is generated from a set number of installations spread over a metropolitan area. In contrast to fossil fuel units, we assume that solar units have zero MC and maintenance and failure probabilities and are continuously scalable. Solar capacity costs are FC^{SL} per MW of capacity, which include installation and scheduled maintenance costs. Solar units are not dispatchable. Production from solar PV generation takes on a state-contingent distribution $n^{SL}\overline{S}$, where $\overline{S} \sim F^S(\cdot|\overrightarrow{w})$. Let $\overrightarrow{F}(\cdot|\overrightarrow{w})$ denote the joint distribution $(F^D(\cdot|\overrightarrow{w}), F^S(\cdot|\overrightarrow{w}))$ of forecasted load and solar output. This formulation allows for the possibility of correlation between forecast errors for demand and for solar generation.

We do not model the possibility that solar generators will be sited distant from existing transmission lines. If renewable facilities are sited far from cities and existing transmission lines—as is often the case with wind but not with solar—then a mandate for increased renewables might imply the need to construct such lines.[15]

In contrast, we assume that a fraction d^{SL} of solar capacity is installed in a distributed environment, which lowers transmission costs in two ways. First, we allow distributed solar to lower the fixed costs of transmission lines. Here, we assume that the discounted present value of equipment investment and maintenance costs is a function of the maximum expected load net of distributed solar:

$$\text{TFC}(n^{SL}) = \text{AFC}^T \max_{\overrightarrow{w}} \{E[\overline{D}(\overrightarrow{w})\overline{p}^{-\eta} - d^{SL}n^{SL}\overline{S}(\overrightarrow{w})]\}, \tag{3}$$

where AFC^T is a parameter and $E[\cdot]$ denotes the expectation operator. From (3), solar production will lower the fixed costs of transmission to the extent that it is positive in hours with the highest load.

Second, we allow distributed solar to lower line losses. Following Bohn, Caramanis, and Schweppe (1984) and Borenstein (2008), we as-

[15] For example, the 290 MW Agua Caliente Solar Project, which went into operation in 2014, is located in southwestern Arizona, right next to an existing 500-kilovolt transmission line.

sume that line losses from transmission in any hour are equal to a constant α times the square of nondistributed generation. Letting Q be load net of demand curtailment and distributed solar generation, line losses satisfy $LL = \alpha(Q + LL)^2$. We let $LL(Q)$ be the function implicitly defined by this relationship and obtain[16]

$$LL(Q) = (2\alpha)^{-1}(1 - 2\alpha Q - \sqrt{1 - 4Q\alpha}). \tag{4}$$

Equation (4) implies that distributed solar production will reduce line losses, especially when it occurs during hours with high load.

D. *System Operator's Problem*

The operator seeks to maximize expected discounted total surplus, subject to $\overline{p}$ and n^{SL}. Her discount factor is β, and the life span for her decisions is T, the life of the generators. Although we have developed our model using a single-agent social optimum approach, our results could be replicated by a competitive market-based model. For example, with multiunit firms, Vickrey auctions for the generation and reserves markets could be used to induce efficient short-run outcomes.[17] Cullen and Reynolds (2016) show that the long-run competitive equilibrium of a generation market will generate the operator's solution; they do not consider reserve operations.

In the first stage, the system operator chooses n^{FF} and p_c. In each second-stage period, the operator makes two decisions conditional on weather forecast $\overrightarrow{w}$, maintenance statuses $\overrightarrow{m}$, and first-stage decisions: (1) generator scheduling decisions $\overrightarrow{on}$ and (2) the amount of demand to be curtailed, z.

We model the choice of operating reserves as a simplified version of how reserves are treated in unit commitment models.[18] Upon learning $(\overrightarrow{w}, \overrightarrow{m})$, the operator chooses on_j for each unit with $m_j = 0$. Then, the state-specific random variables are realized. Possibly a system outage occurs. Otherwise, the operator will adjust generation to exactly match

[16] There are two roots to the quadratic equation. Welfare is maximized at the smaller root.

[17] A Vickrey auction specifies that a firm that sells k units is paid the lowest k losing offers submitted by rival firms (see Krishna 2010). Vickrey auctions are not used by current wholesale markets such as ERCOT, likely because of their complexity. For instance, one would have to have Vickrey auctions for both generation and reserve operations.

[18] A unit commitment model specifies the cost of generation (including start-up costs) as well as costs for several types of reserves: spinning reserve up (to provide for an increased rate of generation), spinning reserve down (to provide for a reduced rate of generation), and nonspinning reserves (see Bouffard, Galiana, and Conejo 2005). Our model is simplified in that we have a single type of operating reserve and no start-up costs, but, in contrast, our reserve policies are endogenously determined.

load by using the generators with the lowest marginal costs to satisfy demand, leaving the generators with the highest marginal costs as reserves. Let $PC(D, \overrightarrow{x})$ denote the ex post minimized costs of power generation and reserves, where D denotes demand (net of curtailment) plus line loss minus solar production, and $\overrightarrow{x}$ denotes generator output realization vectors.

We illustrate the calculation of PC with a simple example. Consider a case with two scheduled generators each with capacity 1, with $c_2 > c_1$, $D = 1.6$, and no generator failures. Following the demand realization, the operator would set output at generator 2 below its full capacity as it has higher costs. Thus, the total production plus reserve costs would be $PC(1.6, (1, 1)) = c_1 + 0.6 \times c_2 + 0.4 \times c_2 \times c^r$.

Let *outage* denote a 0–1 indicator for a system outage. We have

$$\text{outage}(\overrightarrow{on}, z, \overrightarrow{w}) = \mathbf{1}\left\{\sum_{j=1}^{J+n^{FF}} x_j(on_j) + n^{SL}\overline{S} < \overline{D}\overline{p}^{-\eta} - z + LL(\overline{D}\overline{p}^{-\eta} - z - d^{SL}n^{SL}\overline{S})\right\}. \tag{5}$$

In words, (5) indicates that an outage occurs when the maximum realized fossil fuel and solar output is less than demand and line losses net of curtailed demand. Let d^{outage} denote the fraction of customers who lose power times the number of hours for which they lose power in the event of a system outage.

Using these definitions, we now define the system operator's problem for a second-stage period as

$$\begin{aligned} W(\overrightarrow{w}, \overrightarrow{m} | n^{FF}, p_c) = \max_{\overrightarrow{on}, z} & E[[1 - d^{\text{outage}}\text{outage}(\overrightarrow{on}, z, \overrightarrow{w})] \\ & \times [\overline{D}\overline{p}^{-\eta}\text{VOLL} - \text{WLC}(z, p_c)] \\ & - PC(\overline{D}\overline{p}^{-\eta} - z - n^{SL}\overline{S} + LL(\cdot), \overrightarrow{x}(\overrightarrow{on}))|\overrightarrow{w}, \overrightarrow{m}] \\ & \text{such that } m_j = 1 \Rightarrow on_j = 0, \end{aligned} \tag{6}$$

where the expectation is taken over the random variables $F(\cdot, \overrightarrow{w})$ and $\overrightarrow{x}(\overrightarrow{on})$ and the argument of $LL(\cdot)$ is the same as in (5). In (6), the first two lines indicate the gross consumer benefit and the third line indicates the production costs. Generators can be operated only if they are not undergoing scheduled maintenance, which constitutes the fourth line.

We now analyze the stage 1 decisions of p_c and n^{FF}. The system operator rolls up the second-stage payoffs by taking the expected value of W in (6)

over all the hours in 1 year. Let H be the number of hours in a year. Given the stock of generators n^{FF}, the system operator chooses the price for curtailment contracts p_c to maximize expected welfare each year:[19]

$$V(n^{FF}) = \max_{p_c} E[H \cdot W(\vec{w}, \vec{m} | n^{FF}, p_c)], \tag{7}$$

where the random variables are now $\vec{w}$ and $\vec{m}$. Finally, the investment decision for the system operator may be expressed as

$$V^* = \max_{n^{FF}} \left\{ \frac{1-\beta^T}{1-\beta} V(n^{FF}) - n^{SL} FC^{SL} - n^{FF} FC^{FF} - \text{TFC}(n^{SL}) \right\}. \tag{8}$$

The function V^* provides the maximized expected total surplus. It will vary on the basis of the solar capacity n^{SL} as chosen by the regulator.

IV. Data, Estimation, and Computation

A. Data

In order to estimate and calibrate the parameters of our model, we use public data from a variety of sources, notably different federal agencies and grid operators. Our data pertain mostly to a 1-year period from May 2011 until April 2012.

We obtain hourly load data for the Tucson service area from a Federal Energy Regulatory Commission (FERC) Form 714 filing by TEP. Summary statistics on load data are provided in Appendix figure C1. March was the month with the lowest load and August with the highest. Tucson load typically peaks during the summer as a result of high air conditioning use (average August temperature is 88 degrees Fahrenheit). Electricity load in the Tucson area has grown by roughly 1 percent per year.

We draw our data on generation units serving Tucson in 2011 from several sources. The Energy Information Administration (EIA) maintains a database on all existing generation units in the United States. This database includes information about capacity, fuel source, and location. We take from this database the generators owned by TEP, as reported in UniSource (2012).[20] We also use EIA information on the average retail electricity price and capacity investment cost for new generation units.

We obtain information on heat rates from the Environmental Protection Agency's (EPA) eGRID2010 database. This database provides heat

[19] We could equivalently express the problem as one of simultaneous choice of p_c and n^{FF} in stage 1.

[20] TEP has partial ownership stake in four plants, Luna Energy, Navajo, Four Corners, and San Juan, each with multiple generators. For these plants, we assume that TEP owns one generator each with capacity equal to total plant capacity times TEP's ownership share.

rates at the plant level, where a plant may have multiple generation units. We assume that each generation unit at a plant has the same heat rate.

Since our analysis is forward looking, we use information about projected future fuel costs. EIA Form 423 contains information about the terms of multiyear fuel contracts for each of the coal-fired generators. For natural gas we use NYMEX futures prices at Henry Hub in Louisiana (http://www.cmegroup.com/trading/energy/natural-gas/natural-gas.html). We collect the last settlement price for each month for futures contracts in September 2012 for delivery from October 2012 through September 2017. Our natural gas price is the average of these prices.

The eGRID2010 database has mean annual emission rates for CO_2, sulfur dioxide (SO_2), and nitrogen oxide (NO_x) at the plant level. We apply the same emission rates for each generation unit at a plant. Permit fees for SO_2 are from the EPA's annual advance auctions for years 2011–17. TEP units are not subject to NO_x permit fees. The EPA's NO_x Budget Trading program, a cap and trade program for NO_x, applies to 20 eastern states but does not apply to Arizona (see EPA 2011).

We use solar generation data from 58 geographically dispersed installations located within 40 kilometers of the center of Tucson, Arizona. The data were collected by the University of Arizona Photovoltaics Research Lab. They record the power generated (in kilowatts of AC) by each site at 15-minute intervals from May 1, 2011, to April 30, 2012. All installations have fixed-tilt PV panels, mainly facing south. The average system size in the sample is 9.0 (all sizes are in kilowatts of rated DC power), the minimum size is 2.3, and the maximum size is 84.2. Total capacity for the 58 sites is 517 kW. The age of installations (as of the start of the data collection period) ranges from 1 month to 3.5 years, with a mean of 9.5 months. See figure 3 for a map of the installations. The circles represent distances of 10, 20, 30, and 40 kilometers from the center of Tucson. Figure C2 shows the mean and standard deviation of solar output by each 15-minute interval.

A novel aspect of this project is collection and use of weather forecast data, which are used to determine the day-ahead forecasts of load and solar generation. We collect weather forecast data from the National Oceanic and Atmospheric Administration.[21] The forecasts are generally made at 2:00 a.m. and forecast weather for the next day at 3-hour intervals. We interpolate to convert to hourly forecasts. Information includes cloud cover, wind speed, temperature, relative humidity, and dew point. All information is reported as a continuous measure except for cloud

[21] Data are available at http://has.ncdc.noaa.gov/pls/plhas/HAS.StationYearSelect?datasetname=9957ANXsubquery&by=STATION&applname=SRRSBTNSEL&outdest=APPS dtypesort=dtypeord&stationsort=id.

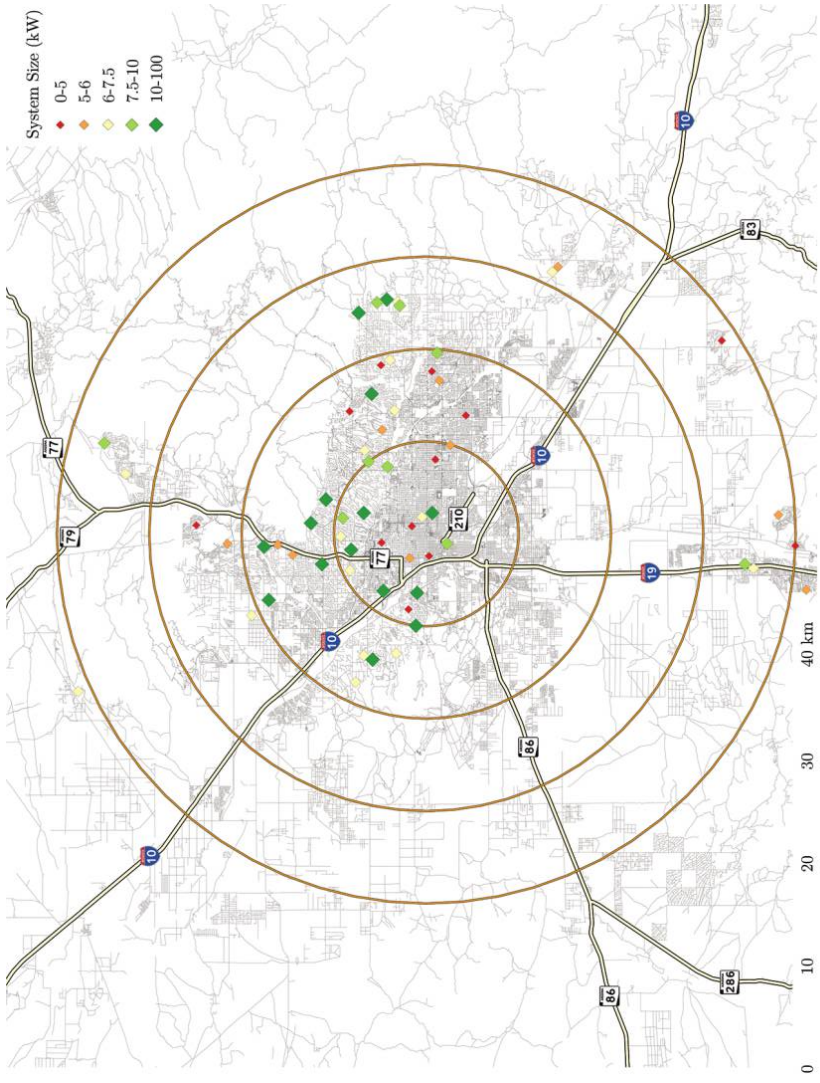

FIG. 3.—Map of Tucson with solar sites in our data. Source: University of Arizona Photovoltaics Research Lab.

cover, which is reported as one of six discrete measures ("overcast" to "clear"), each corresponding to an interval in terms of the numerical percentage of sunlight passing through. We convert cloud cover to a continuous measure using the midpoint of the interval. Our weather forecast data are from the KTUS weather station, located at the Tucson International Airport. We supplement the weather information with data on sunrise and sunset times at the daily level (http://www.timeanddate.com/worldclock/astronomy.html?n=393).

We measure net import quantity as follows. We collect hourly data on generation for all TEP units from the EPA Continuous Emissions Monitoring System database (see EIA 2011).[22] Since some of these units are only partially owned by TEP, we multiply each unit's hourly output by its respective share of TEP ownership. We then calculated the difference between hourly total generation output for TEP and the hourly load to get our measure of net imports. We also obtain a "system λ" for each hour from TEP's FERC Form 714 filing. As this value is meant to reflect the shadow price of additional generation, we use it to proxy for the import price of electricity. Finally, we use data on mean daily temperatures at each weather station in the states of Arizona, California, Nevada, Utah, and New Mexico.

We obtain start-up costs from a National Renewable Energy Laboratory report (see Kumar et al. 2012) that calculates median capital and maintenance costs and associated fuel usage per cold, warm, and hot start-up by generator type and size category. Data for generation unit outages come from the Generating Availability Data System of NERC. These data include outages due to maintenance and forced outages. We use these data for 2007–11 for all US generation units. We obtain data from the United States on system outage durations and number of affected customers from "Major Disturbances and Unusual Occurrences," tables b.1 and b.2 (EIA 2010).

Finally, we use ancillary service auction price data from the ERCOT grid in Texas to define operating reserve costs (ERCOT 2011). Unlike TEP, ERCOT operates a deregulated electricity market with prices. Finally, we obtain total line losses from TEP (see UniSource 2012).

B. Estimation and Calibration of Parameters

Table 1 lists the demand parameters of our base model. Short-run electricity demand is typically estimated to be quite price inelastic (see Espey and Espey [2004] for a survey and meta-analysis). Our value of $\eta = 0.1$ is somewhat lower than the median estimate reported by Espey and Espey but well within their range. Our value of $\overline{p}$ is based on EIA data for Ari-

[22] The generation information for four small natural gas turbine generators with a combined capacity of 108 MW was missing.

TABLE 1
DEMAND PARAMETERS

Parameter	Interpretation	Value	Source
η	Demand elasticity	.1	Espey and Espey (2004)
$\overline{p}$	Retail price per MWh	\$98.10	EIA
g	Demand growth factor	1.20	Based on historical rate of demand growth
VOLL	Value of lost load	\$8,000/MWh	Cramton and Lien (2000)
$F \equiv (F^D, F^S)$	Forecastable distribution of demand and solar output		Estimated

zona in 2011. To be consistent with the loads projected during the middle part of the life of new generation units, we scale demand quantities by $g = 1.2$, based on historical rates of population and electricity consumption growth in Arizona. Importantly, the 20 percent growth yields nonzero investment in new fossil fuel generators for all counterfactuals.

Using mostly customer surveys, Cramton and Lien (2000) report estimates of VOLL that range from \$1,500/MWh to \$20,000/MWh. We choose a fairly conservative estimate of VOLL = \$8,000/MWh (with results from a higher value in table 7 below).

To recover F^D and F^S, we estimate a seemingly unrelated regression (SUR) with load and solar output as the dependent variables. The unit of observation is a 15-minute interval for all daytime hours over our sample period. As solar output is zero at night, we estimate a separate nighttime load regression. We include linear splines and interaction terms of forecast information as regressors. To predict the joint density of solar output and demand, we simulate from the estimated residuals. We use our load estimates to recover the demand constant $\overline{D}$ by inverting the demand equation (1). We trim the solar output at 0 and at the rated maximum capacity.

We follow the approach outlined in Wolfram (1999) and Borenstein, Bushnell, and Wolak (2002) to construct the marginal cost of operation for generation units. We compute the marginal cost of a fossil fuel generation unit as the sum of fuel cost per unit plus SO_2 emissions cost per unit. We report summary statistics for existing TEP generators in table 2. Apart from two small solar PV facilities, all of TEP's generation units are fossil fuel based. We treat the two solar units as though they were dispatchable units producing constantly at full capacity.

Table 2 also lists characteristics of potential new generators. We use a combined cycle natural gas generator with capacity size of $k^{FF} = 191$ MW. This number is the mean of the capacities of 10 planned new units of this type in Arizona throughout 2023 as reported in EIA (2014a). We assume that the other characteristics of new generators are the ones given in the EIA (2013) forecasts of emissions of new plants. For one of the exten-

TABLE 2
SUMMARY STATISTICS FOR TEP GENERATORS, 2011–12

Unit Type	Number of Units	Mean Size	Mean MC	Mean NO_x	Mean SO_2	Mean CO_2
Solar PV	2	6.5 (.5)	0 (0)	0 (0)	0 (0)	0 (0)
Coal	6	263 (133)	23 (10)	3.0 (1.7)	1.6 (1.3)	1.0 (.06)
Natural gas combined cycle	1	185 (0)	35 (0)	.09 (0)	.01 (0)	.4 (0)
Natural gas steam turbine	3	89 (13)	54 (0)	1.5 (0)	.03 (0)	.5 (0)
Natural gas turbine	6	39 (20)	71 (13)	3.5 (2.0)	.05 (.01)	.8 (.2)
Potential new natural gas combined cycle	. . .	191	32.60	.05	.01	.4
Potential new natural gas turbine	. . .	91	47.60	.31	.01	.5

SOURCE.—Authors' calculations based on a variety of data sources.

NOTE.—Standard deviations are in parentheses. MC figures include emissions permits. Size is measured in MW, MC in dollars per MWh, NO_x and SO_2 emissions in pounds per MWh, and CO_2 emissions in tons per MWh.

sions of the model, we also allow for potential new natural gas turbine generators. We also use the mean size of these planned units for Arizona, which is 91 MW.

We calculate start-up costs by multiplying the extra reported fuel used for start-ups by our fuel prices and adding the reported capital and maintenance costs to obtain our start-up cost measure. Appendix table C1 provides details on our calculated start-up costs for generators in our sample. These match closely with the start-up costs for Spanish electricity generators estimated by Reguant (2014).[23]

A key input into our analysis is the installed cost per unit of solar PV capacity. On the basis of results for 2012 from Barbose et al. (2013), we find that the installed cost is $3.93 per W of DC power.[24] We add the net present value of the cost of replacing inverter equipment, to arrive at a capacity cost of $4.41 per W of DC power.[25]

Table 3 lists solar PV capacity cost and the remaining supply parameters. We compute the ratio of the hourly reserve marginal cost to the hourly generation marginal cost, c^r, using data from the deregulated ERCOT market on the 2008 prices in the up-regulation and responsive

[23] Another potential cost is ramping costs, which are the costs of changing output. Reguant (2014) finds that the costs of ramping a substantial amount over 1 hour, 100 MW, are vastly lower than the costs of starting up a unit. Hence we do not account for ramping costs.

[24] Using data for 2012, Barbose et al. (2013) report a US average installed cost of $3.30 per W of DC for utility-scale projects (>2 MW) and an average installed cost of $5.40 per W of DC for distributed PV projects in Arizona (based on their table B-3). These installed costs are averaged using the Arizona standard that a fraction $d^{SL} = .3$ of solar PV capacity must be distributed generation.

[25] Following Baker et al. (2013), we assume that inverter equipment is priced at $0.60/W, real inverter prices fall by 2 percent per year, and inverters are replaced twice over the life of the modules.

TABLE 3
REMAINING SUPPLY PARAMETERS

Parameter	Interpretation	Value	Source
d^{outage}	System outage hours times % of affected customers	.98	EIA
d^{SL}	Fraction of solar generation that is distributed	.3	Arizona Renewable Portfolio Standard
FC^{FF}	New combined cycle gas generator capital cost per MW	$1,095,458	EIA
FC^{FF}	New gas turbine gas generator capital cost per MW	$921,927	EIA
FC^{solar}	Solar capital cost per MW of DC	$4,410,000	Baker et al. (2013), Barbose et al. (2013)
c^r	Ratio of MC for operating reserves to production MC	.41	Calculated from ERCOT data
α	Line loss constant	.000035	Calculated fromTEP Form 10K
AFC^T	Average transmission fixed cost per MW	$1,259,000	Baughman and Bottaro (1976), Borenstein and Holland (2005), and TEP line loss cost
β	Discount factor	.94	
T	Lifetime of generators in years	25	

reserve markets, which pay firms in exchange for giving ERCOT the option to force them to operate with short notice.[26] If they operate, they receive the price on the balancing market. The average price is $65.41/MWh in the balancing (production) market, $27.05 in the responsive reserve market, and $22.71 in the up-regulation market. The average of the ratio of the responsive reserve market to balancing market prices over all hours is 0.42, while the average of the ratio of the up-regulation to balancing market prices over all hours is 0.40. Our estimate of the reserve costs is the average of these two numbers.

We estimate the transmission cost parameters as follows. For line losses, we find the value of α that matches TEP's reported line losses of 6.6 percent of 2011 load, using $LL(Q)$ defined in equation (4) to calculate line loss as a function of α in any hour and then summing across every hour in 2011 to get total line losses as a function of α. To calculate AFC^T, we approximate average generating costs by $70/MWh, so that the 6.6 percent line loss represents $4.62/MWh. We difference the line loss from the total transmission and distribution (T&D) cost of $40/MWh from Borenstein and Holland (2005) to obtain an average T&D fixed

[26] The up-regulation market gives firms 3–5 seconds to adjust production while the responsive reserve market gives 10 minutes.

cost of \$35.38/MWh. Using information in Baughman and Bottaro (1976), we calculate that 55.3 percent of T&D fixed cost can be attributed to transmission. We obtain AFC^T in (3) by multiplying 55.3 percent of \$35.38 by the discounted sum of expected load and then dividing by the maximum expected load.

To estimate d^{outage}, we use major disturbances reported by EIA (2010) whose causes were due to equipment failure (not, e.g., due to storms) that affected more than 50,000 customers. For 2008 there were 21 such disturbances for which we could find both the total number of customers and the number of affected customers, from which we calculate the percentage of customers affected. For each of the 21, we multiplied the duration by the percentage of customers affected. We estimate d^{outage} as the mean of this product.[27]

We calculate generator maintenance probabilities as the ratio of the number of occurrences of outages due to maintenance to total available hours; for failure probabilities we use forced outages. We compute maintenance outage and forced outage probabilities separately for coal units and for natural gas units. We report the probabilities in table 4. Note that coal generators report a higher P^{fail} than do gas generators.

C. *Computation of the System Operator's Problem*

We compute the system operator's problem conditional on a solar capacity level n^{SL} by finding the values of the long-run choice variables, n^{FF} and p_c from (8) and (7), respectively, that maximize social welfare. Since n^{FF} is a discrete variable, we perform a grid search for this variable and a search using the simplex method for p_c.

The social welfare of any long-run choice depends on the discounted sum of the welfare levels at each hour in the T-year life span of the generators, net of the fixed costs. The observable datum (to the economist) for an hour is the weather forecast, $\vec{w}$. We assume that the weather forecasts for the year-long sample period are repeated for each of the T years. The operator also observes maintenance status $\vec{m}$, and we integrate over this variable with simulation as it is not observed.

For a given hour, observing $(n^{FF}, p_c, \vec{w}, \vec{m})$, the operator chooses $\overrightarrow{on}$ and z. For each value of $(n^{FF}, p_c, \vec{m}, \vec{w}, \overrightarrow{on}, z)$, we simulate generator failures $\vec{x}(\overrightarrow{on})$ and demand and solar output $F(\cdot, \vec{w})$ and solve for the social welfare at that hour. We then perform a grid search in $\overrightarrow{on}$ and z to maximize social welfare at that hour. For each n^{FF} and p_c, we sum the maximum welfare levels across $(\vec{w}, \vec{m})$ to obtain the total welfare that feeds into our simplex search.

[27] Our estimate here is an approximation because some of these system outages may be due to failure of equipment other than generators.

TABLE 4
MEAN HOURLY MAINTENANCE AND FAILURE PROBABILITIES

	Failure Probability, P^{fail} (%)	Maintenance Probability, P^{maint} (%)	Mean Number of Units per Hour
Natural gas generator	.0492	.0382	342
	(.01)	(.008)	
Coal generator	.099	.047	859
	(.027)	(.010)	

SOURCE.—Generating Availability Data System of NERC.
NOTE.—The time period covered is 2007–11. Standard errors are in parentheses.

We make a couple of simplifications to our short-run optimization algorithm, in the interest of computational tractability. First, we assume that the operator schedules generators in ascending order of MC when computing optimal generation for a second-stage period.[28] Although this point is intuitively reasonable, because of differences in sizes and failure probabilities across generators, it is possible that a system operator would want to schedule a higher-MC generator and not a lower-MC one. Second, we assume that the operator curtails demand only if all available generators for which MC is below the marginal cost of curtailment, $d\text{WLC}(z)/dz$, are scheduled. Again, this point is intuitively reasonable but may not hold exactly because generators come in discrete chunks.

We now provide some details on the simulation procedures. We use 20 draws to simulate from the estimated residuals of the joint distribution of load and solar output conditional on a forecast. Note that the operator's problem also involves simulation of generator failures. Failure probabilities for individual generators are small, and probabilities of multiple failures—which might cause a system outage—are very small, but the adverse consequences of a system outage are very large. Thus, our computation is challenging because integration using a direct simulation method would be very inefficient. Instead, for each type of generator, we integrate over the probability of a given number of failures given a total number of generators operating and then simulate the identity of failed generators conditional on the number of failures. We integrate over maintenance probabilities using the same method.

Finally, note that our results compare the baseline to a number of different counterfactual environments. To minimize the impact of simulation error on our results, we use the same demand, solar output, maintenance, and failure simulation draws for all environments when possible. For the counterfactuals in which we use different forecasting technology (e.g., afternoon weather forecasts instead of morning ones), we cannot

[28] This is called "sequential optimization" in the electricity literature (see Independent Electricity System Operator 2012).

use the same distribution of predicted residuals for demand and solar output as in the baseline. Here, we normalize the simulated draws so that the mean demand and solar output are the same as in the baseline.

V. Results

We first discuss the results of our forecast estimation. We then analyze the baseline predictions of our model, break down the sources of social costs for solar energy, and evaluate the social costs of solar energy under different complementary environments.

A. Forecast Estimation Results

The estimated relationship from the SUR model of daytime load and solar output on weather forecasts is reported in Appendix table C2. The nighttime impact of weather forecast on load is reported in Appendix table C3.

We find a U-shaped relation between forecasted temperature and load in both regressions, which occurs because electricity is used for both heating and cooling. For solar output, forecasted cloud cover variables are negative and are increasing in magnitude with more cloud cover, as expected. The R^2's are .959, .945, and .878 for daytime load, nighttime load, and solar output, respectively. The correlation in the residuals between load and solar output is .093 and is statistically significant ($\chi^2(1) = 152$, $P = .00$).

Given that we assume that the system operator can use our regression output for generator scheduling and demand-side management, it is useful to understand how the precisions of our forecasts compare to those used by electricity firms and in the systems engineering literature. While we could not obtain TEP forecast information, Hydro One, the largest electricity provider in Ontario, reports R^2 values between .84 and .92 for their load predictions (Hydro One 2012). Many engineering studies report the mean absolute percentage error (MAPE), defined as the mean of the absolute value of load minus predicted load all divided by load, rather than R^2. Our daytime and nighttime MAPEs are both 0.03. A variety of studies on forecasting report MAPEs for load that range from 0.017 to 0.027 (see Weron and Misiorek 2004; Fay and Ringwood 2010).

For solar, MAPE will be infinite because output can be zero. It is common to report the relative root mean squared error (rRMSE) here, which is the square root of mean squared forecast error, divided by mean output. We find a daytime rRMSE of 0.23. This compares to daytime rRMSE values of 0.17–0.46 reported from a variety of solar studies using several different forecasting models (see Larson 2013). Thus, we believe that our forecast precision—for both load and solar output—is well within the range of forecasts that are currently used by utilities.

B. *Social Costs of Large-Scale Solar Energy*

Table 5 reports our computational results for the social costs of large-scale solar generation, with more details in Appendix table C4. The first column reports the baseline with no solar PV investment. The remaining columns progressively add more solar capacity up to 20 percent of generation being produced by solar. Overall, we find that the social cost of large-scale solar energy—not accounting for CO_2 benefits—ranges from \$126.70 to \$138.40 per MWh.

Comparisons between solar PV and conventional generation are often based on levelized cost, which is the average cost over the life of the unit. The realized solar output and our assumption about the cost of solar panels together yield a levelized cost of \$181.20 per MWh for solar PV generation. The levelized cost for a new combined cycle generation unit is \$66.30 per MWh (see EIA 2014b). Thus, on the basis of a simple average cost comparison, solar PV imposes an additional per-unit cost of \$114.90 per MWh. Our analysis, which endogenizes choices in response to a solar mandate, finds that the social costs of 20 percent solar penetration are higher than the levelized cost difference by \$23.50 per MWh.

We now evaluate the predictions of our model in a little more depth. Building solar capacity causes the system operator to forgo natural gas generators. While the number of new gas generators is weakly monotonically decreasing in solar output, the decrease is very nonlinear, with the planner forgoing two generators with 10 percent or 15 percent solar and three generators with 20 percent solar. For the 20 percent solar case, the three gas generators have a combined capacity of 573 MW, while the listed solar capacity is 1,881 MW.

TABLE 5
THE SOCIAL COSTS OF LARGE-SCALE SOLAR (Base Specification)

	Fraction of Generation from Solar			
	0%	10%	15%	20%
Forgone new gas generators (N)	0	2	2	3
Mean system outage probability	4.76e−5	5.82e−5	5.81e−5	8.4e−5
Reserves (as % of energy consumed)	30.5	32.1	33.6	35.2
Curtailment quantity (as % of total load)	.11	.19	.14	.24
Curtailment price p_c (\$/MWh)	661	469	431	804
Production costs	437.20	380.00	355.20	332.20
Reserve costs	78.10	81.50	82.80	84.80
Gas generator investment costs	2,090	1,672	1,672	1,463
Solar capacity investment costs	0	4,148	6,221	8,295
Transmission fixed costs	331.40	319.40	317.40	316.20
Loss in \$ surplus per MWh solar produced	. . .	126.70	133.70	138.40
Loss in \$ surplus per ton CO_2 reduced	. . .	293.10	283.50	279.10

NOTE.—Cost variables are measured in millions of dollars per year. The row for loss in \$ surplus per MWh solar produced does not account for environmental benefits except for SO_2 permits.

A system outage occurs with probability 0.0048 percent each hour in the baseline, rising to 0.0084 percent with 20 percent solar. NERC mandates a "1 day in 10 years" standard for system outage. The interpretation of the NERC standard varies across utilities (see Cramton, Ockenfels, and Stoft 2013). If the standard is interpreted as "one event in 10 years," then this corresponds to a system outage probability of 0.0011 percent for each hour. If it is interpreted as "24 hours of system outage in 10 years," then it corresponds to an expected failure probability of 0.027 percent in any hour. Our model uses a mean system outage duration of 4 hours implying an analogous figure of 0.019 percent for our model. Thus, depending on the interpretation, our model predicts a baseline optimal failure probability that is either 30 percent lower or four times higher than the NERC outage standard. Moreover, the optimal outage probability rises significantly but not dramatically given large-scale solar.

On average over all hours, operating reserves are 30.5 percent of load with 0 percent solar, going up to 35.2 percent for the 20 percent solar case. Thus, our predicted reserves for 0 percent solar are higher than the 23 percent ratio necessary to meet NERC reserve standards (noted in Sec. II.A). Given that we use an approach for choosing reserves that differs from the NERC criteria, we would not expect predicted reserves to match the 23 percent benchmark. Extra reserves may also arise because we approximate the scheduling problem with sequential optimization, whereby the operator turns on generators solely in increasing order of marginal cost. Even though reserve operations increase with the solar penetration, this effect adds only $6.7 million in annual costs for 20 percent solar relative to the baseline. This is, for instance, far less than the decrease in production costs ($105 million) over this range.

Baldick et al. (2006) report that prices for curtailment contracts range from $150 to $600 per MWh. The comparable price for our baseline is $661 minus the retail price of electricity, or $563 per MWh. Thus, our baseline number is within the range that exists in the real world.

We find that the probability of some demand curtailment in July at 6:00 p.m. rises monotonically with solar penetration, from 9.7 percent without solar to 58 percent with 20 percent solar. July at 6:00 p.m. is a time of moderately high demand but low solar output. In contrast, the probability of some demand curtailment in July at noon goes down monotonically with more solar output. Overall, the curtailment quantity and price chosen are not monotonic in solar output, though both are higher with 20 percent solar than with no solar. Here, the multiple trade-offs between solar generation, backup fossil fuel generation, system outage probability, and curtailment do not lead to an easily quantifiable trend.

We find that the probability of having at least one gas generator scheduled goes down from 97 percent to 90 percent as we go from 0 percent or 10 percent solar to 20 percent solar and that the social costs of solar

increase over the 10–20 percent range. Borenstein (2008), Lamont (2008), and Joskow (2011) point out that valuation of a renewable generation source should be based on the marginal cost of the generation it displaces. Since coal generators have lower marginal costs, the fact that solar substitutes more from coal at higher capacity levels contributes to the increase in the social costs of solar as solar capacity increases.

Table 5 also compares the loss in social surplus from each solar policy relative to the baseline to the offset CO_2 emissions. We find that the dollar cost per ton of CO_2 reduced ranges from \$293.10 with 10 percent solar penetration to \$279.10 with 20 percent solar penetration. The US government baseline value for the social cost of CO_2 in 2015 is \$39 per ton (EPA 2015). Thus, using our capital cost numbers, one could not justify large-scale investment in solar on a social cost basis using the US government figures. However, solar capital costs have been dropping dramatically and are expected to drop further. For this reason, we expect this result to change over time. Figure 4 considers the social break-even point for 20 percent solar as a function of solar capital costs. We find that solar capacity costs would have to drop to \$1.52 per W for 20 percent solar to be welfare neutral at the central 2015 US government figure or to \$2.43 per W for welfare neutrality at the 95th percentile figure (EPA 2015).[29]

Finally, Appendix table C5 examines the social costs of solar including start-up costs of fossil fuel generators. We find that adding large-scale solar does add to the total costs of start-ups. For instance, with 20 percent solar penetration, the total costs per start-up account for an increase in \$5.30 per MWh of solar generated, raising the social cost of solar from \$138.40 per MWh to \$143.70 per MWh. Note that this likely overstates the extra start-up costs generated by large-scale solar as, in our model, the system operator does not account for these costs in making her decisions.

C. Components of Social Costs for Solar

Table 6 decomposes the sources of the social costs of 20 percent solar. The first row repeats the base 20 percent solar case from table 5. The next four rows examine the impact of different components of intermittency on the social costs of solar. First, we find that eliminating the

[29] The displacement of fossil fuel generation displaces other pollutants besides CO_2. Our analysis accounts for part of this benefit by including the EPA permit price for SO_2 emissions. However, the recent SO_2 permit price we use is close to zero and likely understates the marginal damage of SO_2 emissions (Schmalensee and Stavins 2013). Muller and Mendelsohn (2009) estimate marginal social damages from SO_2 and NO_x. Using their values, we nonetheless find very small benefits to solar from offset emissions of these pollutants.

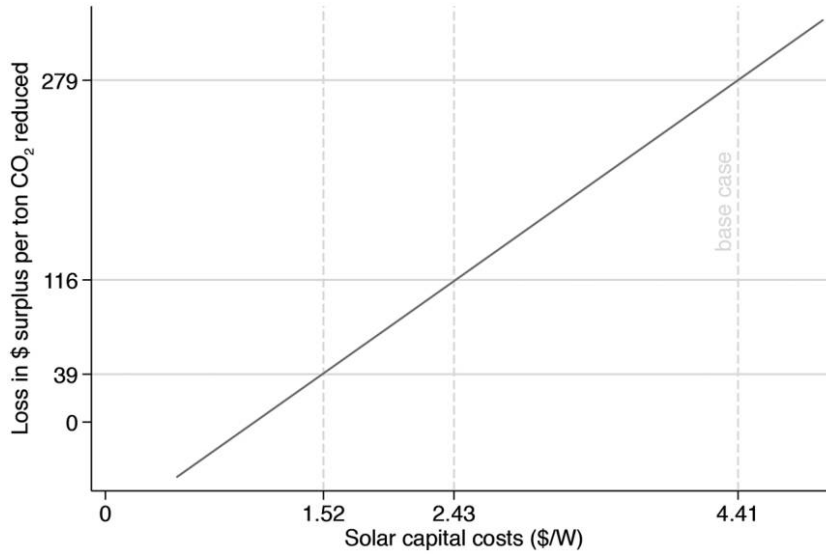

FIG. 4.—Solar capital costs versus social costs for 20 percent solar. Our baseline solar capital cost is $4.41, $39 is the EPA mean social cost of carbon, and $116 is the 95th percentile social cost of carbon, both using a 3 percent discount rate. Color version available as an online enhancement.

unforecastable component of solar output lowers social cost by $6.10 per MWh relative to the base case. This drop is small compared to the overall additional social cost of solar generation. System engineering studies that account for backup capacity and operating reserve changes often find higher costs of unforecastable intermittency,[30] while studies that employ a narrower set of cost factors find somewhat lower costs.[31]

We next consider the total intermittency costs, which we define to be the difference in social costs between large-scale solar and a perfectly dispatchable energy source that produced the same total output.[32] We find that perfect dispatchability would lower the social cost of 20 percent

[30] For instance, Skea et al. (2008) find a cost of roughly 15 percent of the cost of wind generation for 20 percent wind power penetration in the United Kingdom. This figure is based on the difference between the capacity credit for wind and average wind production. The capacity credit of a generation resource is meant to capture its contribution to system reliability and hence is similar to our notion of unforecastable intermittency.

[31] For 9–17 percent solar PV penetration in the Arizona Public Service (Phoenix) territory, Mills et al. (2013) estimate that eliminating PV forecast errors would reduce costs by $2–$4 per MWh of solar generation. Their analysis does not adjust backup generation, for instance.

[32] The systems engineering literature has no single accepted definition for total intermittency costs, or, as it is often called in this literature, integration costs. A common approach is to define integration costs as the difference between total system cost with renewables and total system cost for a reference case without renewables, although such a definition depends on how the reference case is defined (Milligan et al. 2011).

TABLE 6
DECOMPOSITION OF SOCIAL COSTS OF 20 PERCENT SOLAR

Experiment	Loss in $ Surplus per MWh Solar	Number of New Gas Generators	Curtailment Price p_c ($/MWh)
Base case—feasible solar	138.40	7	804
No unforecastable intermittency	132.30	7	792
Fully dispatchable	92.40	1	300
Equal generation profile	133.80	7	783
Eliminate distributed generation: $d^{SL} = 0$	118.70	7	834
Fixed costs FC^{SL} drop from $4.41/W to $2/W	39.40	7	804
Same policies as without solar	281.60	10	661
Rule-of-thumb policy with 10% solar capacity credit	154.80	10	661
Rule-of-thumb policy with 12.5% solar capacity credit	153.20	9	661

NOTE.—"No unforecastable intermittency" produces at the forecastable mean. "Fully dispatchable" solar can be dispatched on the basis of the demand forecast. "Equal generation profile" produces equally at every hour with the same total capacity as the baseline. "Rule-of-thumb" policies reduce fossil fuel capacity by the capacity credit of installed solar capacity and increase daytime reserves until the mean system outage probability is the same as in the base case.

solar by a substantial $46 per MWh, in part by having the planner build six fewer generators. While many factors together result in the relative unimportance of unforecastable intermittency, it is worth noting that the R^2 of .878 for solar output is very similar to the ratio of 0.867 of forecastable to total intermittency costs.

A hypothetical solar facility that always produced at its mean output level would be better than the base case by $4.60 per MWh. Distributed generation is also costly, raising the cost of solar by $19.70 per MWh. Here, the transmission cost savings from distributed generation are small relative to the extra capacity costs.

All of these savings are small compared to the fixed cost of solar. Our fixed cost of $4.41 per W reflects average installed costs in 2012 for a mix of utility-scale and distributed (residential and commercial) sites, but the lowest-cost utility-scale projects in the United States were approximately $3.00/W of DC power (including costs of inverter replacements; see Barbose et al. 2013). If the cost of solar were to drop to $2 per W as many industry observers believe will occur, then the social costs of large-scale solar would drop by $99 per MWh.

The final three rows of table 6 compare the social cost of solar under alternative policy environments. We first examine a policy in which the system operator uses the same n^{FF} and p_c as in the base case and, in each

stage 2 period, employs the same quantity of operating reserves and curtailed demand.[33] We find that this policy results in a much higher social cost of large-scale solar: $281.60 per MWh instead of $138.40 in the base case. Part of the reason is the extra generator cost. Not reported in table 6, much of the loss comes from a much higher system outage probability than in the base case, of 0.3 percent in each period.

We also examine social costs in which the system operator adjusts capacity and reserve operations using rules of thumb similar to those suggested by the systems engineering literature. First, we assume that the system operator reduces gas generator capacity by the solar *capacity credit*, which indicates the percentage of the solar capacity that is reliably available to meet load during peak demand periods. Utilities in the southwestern United States use solar capacity credits that range from 11.7 percent to 14.4 percent (Sigrin et al. 2014, table 1). Mills and Wiser (2012a, 2012b) and Sigrin et al. (2014) all note that simulation studies of reliability yield lower capacity credits for solar PV as PV penetration rises. We consider two different capacity credits: 12.5 percent (which is roughly the midpoint from Sigrin et al.) and 10 percent (which lowers this number to account for the higher PV penetration in our study).[34] Second, we assume that system operators would preserve the same mean system outage probability as in the baseline by increasing reserve operations by a fixed amount in all daytime hours until the mean system outage probability matches the baseline level.

We find that both rule-of-thumb policies have social costs that are about $15 per MWh higher than under the optimum, implying that reoptimization may be important in lowering social costs of renewable energy. More generally, utilities often express concern over the costs of integration for large-scale renewable energy. We believe that the reason for this may be that they are not sure of how policies should optimally change in the case of large-scale solar. The envelope theorem implies that it is not necessary to reoptimize policies with only a small amount of solar on the grid. But the envelope theorem no longer holds with 20 percent of electricity generation from solar. Thus, a very useful complement to large-scale renewable energy is policy reoptimization with the goal of minimizing social costs.

D. Robustness to Environment

We now examine how the social cost of solar changes across different environments, with results in table 7 and figure 5. The first row of table 7

[33] Since reserve operations come in discrete quantities, we cannot implement exactly the same reserve operations. We use the smallest level of reserve operations that is weakly greater than in the base case.

[34] Both are lower than the solar capacity factor (mean production level per unit of capacity) in our data, which is 20.1 percent.

TABLE 7
SOCIAL COSTS OF 20 PERCENT SOLAR GIVEN DIFFERENT ENVIRONMENTS

ENVIRONMENT	SURPLUS WITHOUT SOLAR (Million $/Year)	LOSS IN $ SURPLUS PER MWH SOLAR	NUMBER OF NEW GAS GENERATORS		CURTAILMENT PRICE p_c ($/MWh)	
			No Solar	20% Solar	No Solar	20% Solar
Base environment	134,481	138.40	10	7	661	804
No interruptible power contracts	134,453	137.80	12	10	. . .	. . .
Imports and exports allowed	134,508	139.20	10	8	. . .	. . .
Investment in additional generator type (see note)	134,482	138.40	8 (CC) 3 (GT)	6 (CC) 3 (GT)	677	696
2 p.m. (instead of 2 a.m.) forecasts	134,482	139.30	10	8	701	488
Forecasts with 24-hour lagged demand	134,485	138.50	10	7	600	1,020
VOLL increased to $12,000	202,225	138.90	10	8	661	469

NOTE.—"Investment in additional generator type" allows the system operator to invest in both natural gas combined cycle (CC) and natural gas turbine (GT) generators. All other specifications allow investment only in combined cycle generators.

repeats the base environment, now presenting both the total surplus in the absence of solar and the change in surplus per MWh solar output for 20 percent solar. The second row presents the case without curtailment contracts. In this case, the baseline welfare goes down by about $28 million per year. But the loss in surplus from 20 percent solar is almost the same in the base environment and without curtailment contracts. The net effect is that the social cost of solar is virtually unchanged from the base environment, at $137.80 instead of $138.40 per MWh solar.

A similar pattern is repeated across all rows in table 7. The third row examines the value of adding imports and exports, which we obtain by first estimating a net import function and then by solving the operator's problem with the estimated net import function.[35] With imports and exports allowed, the baseline welfare increases by $27 million per year, but the social cost of solar is very similar to that of the base environment, although net exports increase substantially in the presence of 20 percent solar production. The assumption of no imports or exports has been used in other studies of electricity in the western United States (see, e.g.,

[35] We follow the estimation method of Bushnell, Mansur, and Saravia (2008) here. See App. B for details on the estimation and model.

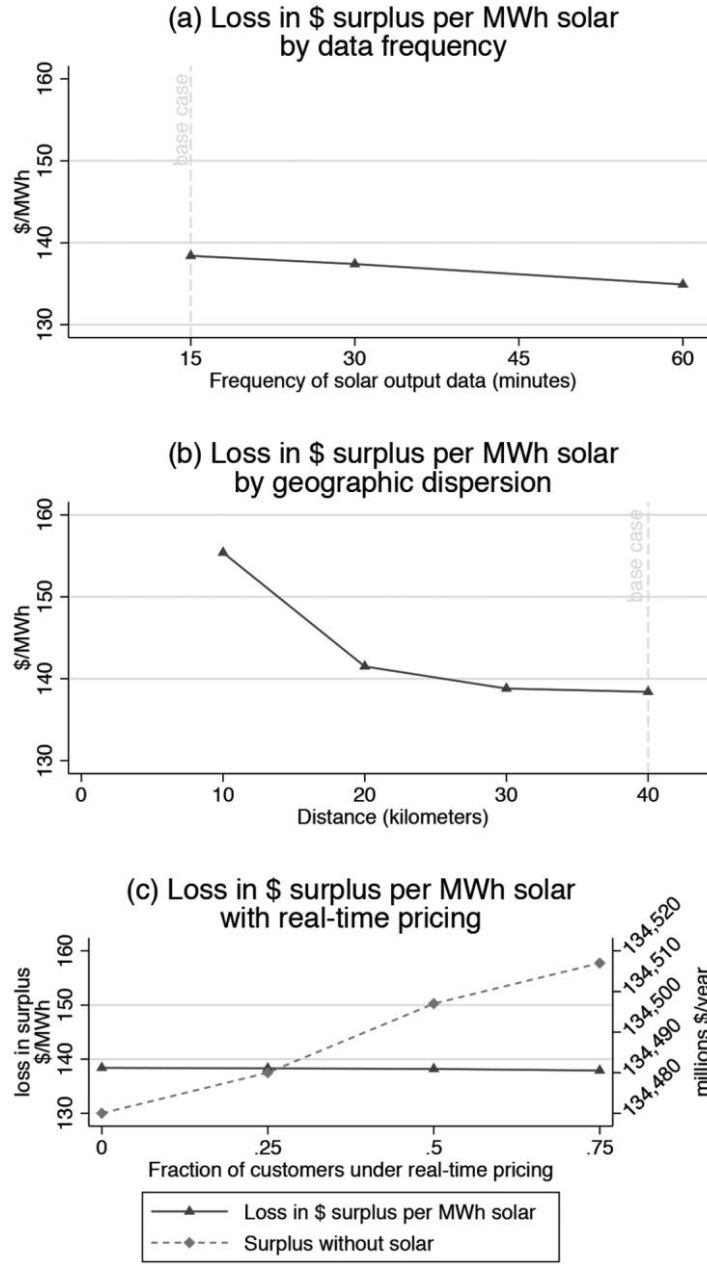

FIG. 5.—Social costs of 20 percent solar from unforecastable intermittency, geographic dispersion, and real-time pricing. Color version available as an online enhancement.

Borenstein and Holland 2005; Mills et al. 2013). While these studies measure a wider geographic area, our results show that this assumption does not have a large impact on solar valuation for even the relatively small area that we consider. An important caveat is that, by holding constant the current import elasticity into the future, we are essentially assuming that TEP expands solar while other utilities do not.

We next examine the impact of allowing the system operator to choose two types of new gas generators: combined cycle and gas turbine. The values from this change in environment, both with and without solar, are very modest. However, the system operator does choose some gas turbine generators. For instance, with 20 percent solar, the system operator goes from building seven new combined cycle generators under the base environment to building six combined cycle and three (smaller) gas turbines when allowed.

We next consider the value of better forecasts and again find little change in value. Finally, table 7 examines the impact of increasing the value of lost load from \$8,000 to \$12,000. The higher VOLL causes a huge increase in the total welfare but changes the social cost of solar by only a tiny amount, \$0.50 per MWh. Even though the loss in surplus from 20 percent solar is similar across all the environments that we consider, the optimal curtailment price with 20 percent solar varies quite a bit, from \$469 to \$1,020, for the environments with demand curtailment.

Figure 5 shows the impact of three more types of environment. Part *a* shows the impact of the intermittency costs as the time scale of solar output observations increases.[36] We find a \$3.50 decrease in the social cost of solar per MWh with 60-minute data. Our results on the impact of the solar generation time scale are roughly consistent with results in Mills and Wiser (2010). Thus, the high-frequency nature of solar intermittency adds costs.

Our baseline analysis uses data from 58 solar sites within 40 kilometers of the center of Tucson. Part *b* of the figure shows the impact of having fewer, more geographically concentrated sites on the social cost of high solar penetration. Here, we find that the results are quantitatively important: having only sites within 10 kilometers of the center results in social costs that are \$17 per MWh higher than the baseline. Relatedly, the R^2 of the solar forecast increases monotonically from .866 with the 10-kilometer radius to .878 with the 40-kilometer radius. By including all sites within 20 kilometers of the center, the social costs are very similar to the 40-kilometer costs. As a caveat, we note that we are comparing sites that may use slightly

[36] Appendix B provides modeling details for the model with multiple solar observations per hour.

different solar technologies and have different environmental characteristics, such as shade prevalence.

Finally, part *c* of figure 5 shows the impact of real-time pricing contracts on the social cost of solar.[37] Adding customers on real-time pricing adds to the social value. For instance, without solar, having 75 percent of customers on real-time pricing contracts adds $36 million to annual social surplus relative to having no real-time pricing (the dashed line). Yet, a very similar total benefit of real-time pricing arises in the presence of solar. Thus, real-time pricing has a negligible effect in changing the social costs of large-scale solar.

VI. Conclusions

A variety of current and potential policies have stimulated investment in renewable energy generation. Intermittency of renewable generation may have a significant impact on electric grid reliability, system operations, and requirements for backup generation capacity. Because a grid operator must make different long- and short-run decisions in response to intermittent renewable output, we believe that the social costs of intermittency can best be understood in the context of a model that maximizes welfare.

We develop an empirical approach to estimate the social costs of renewable energy accounting for their intermittent nature. Our approach has three parts: (1) a theoretical model that is based on the work of Joskow and Tirole (2007), (2) a process to estimate and calibrate the parameters of this model using publicly available data, and (3) a computational approach to evaluate the impact of counterfactual policies and environments.

The biggest limitations of our approach are that we do not optimize over dynamic linkages from period to period and that we do not consider market power, evaluating only the social optimum.[38] Moreover, our assumed operating reserve costs are at best an approximation of reality.

We examined the impact of large-scale solar on the Tucson, Arizona, grid area. We find that the social costs of 20 percent solar generation are $138.40 per MWh of which unforecastable intermittency accounts for only $6.10 per MWh. While these numbers pertain to only one metropolitan area, evidence from solar potential maps and output and load at dif-

[37] In our model, the system operator chooses the prices for these contracts at the same time as she schedules generators, 1 day in advance. Appendix B provides modeling details for this model also.

[38] Cullen (2010a) estimates a dynamic model of start-up costs for generators. A similar model would hugely complicate our analysis.

ferent sites throughout the United States suggests that the social costs would be similar for the southwestern quadrant of the United States. Other environments, such as allowing imports and exports outside of the grid area or allowing a greater fraction of consumers on real-time pricing contracts, have very small impacts in terms of changing the social costs of large-scale solar.

Our study has a number of broader implications beyond the results for solar generation in Arizona. First, our finding that the costs of intermittency for solar energy are lower than many industry observers believe may be important. In particular, costs associated with intermittency are a relatively small component of the overall welfare cost of large-scale solar; the bulk of the welfare cost is simply the high installation cost of solar. Our results on intermittency stem from the assumption that utilities implement substantial changes in demand-side management policies, reserve operations, and investment in backup fossil fuel generators in response to substantial solar capacity. It is possible that utilities need to obtain knowledge about how these decisions should change in the presence of substantial renewable generation, and our study provides a framework that can be used to guide utilities along this dimension.

Second, our study has implications about the benefits of different renewable energy policies. While we find that an immediate investment in large-scale solar with current technology would reduce welfare, if solar capacity costs drop below \$1.52, large-scale solar PV generation becomes welfare increasing when accounting for the benefit from offset CO_2 emissions.

Finally, our approach can be used to analyze a variety of other energy policies, many of which might require changes in complementary policies to minimize social costs. These policies include understanding the social costs of reducing emissions from a renewable energy standard versus a carbon tax and how technologies such as battery storage and electric cars that change the effective time pattern of demand can change the value of renewable mandates.

Appendix A

Derivations of Demand-Side Properties

LEMMA 1. With demand specified in (1) and retail price fixed at $\bar{p}$, VOLL is constant across states. The relation between VOLL and v is monotonic and satisfies

$$v = [(1 - \eta)\bar{p}^{-\eta}\ \text{VOLL} + \eta\bar{p}^{1-\eta}]^{1/(1-\eta)}. \tag{A1}$$

Proof.

$$\begin{aligned}\text{VOLL} &= \frac{\int_{\overline{p}}^{v} D(p,\overline{D})dp + \overline{p}D(\overline{p},\overline{D})}{D(\overline{p},\overline{D})} \\ &= \frac{\overline{D}\left(\frac{1}{1-\eta}\right)(v^{1-\eta} - \overline{p}^{1-\eta}) + \overline{p}\overline{D}\overline{p}^{-\eta}}{\overline{D}\overline{p}^{-\eta}} \\ &= \frac{\overline{D}\left(\frac{1}{1-\eta}\right)(v^{1-\eta} - \eta\overline{p}^{1-\eta})}{\overline{D}\overline{p}^{-\eta}} \\ &= \frac{v^{1-\eta}\overline{p}^{\eta} - \eta\overline{p}}{1-\eta}.\end{aligned}$$

Solving for v in terms of VOLL and the other parameters, we obtain the expression in the statement of the lemma.

LEMMA 2. Assume that the demand that can be curtailed in any period is limited by the minimum demand scale, $\overline{D}^{\min}(\overrightarrow{w})$. If $p_c < v$, then curtailment quantity is bounded above by $\overline{D}^{\min}(\overrightarrow{w})(\overline{p}^{-\eta} - p_c^{-\eta})$. The welfare loss associated with curtailment quantity z is

$$\text{WLC}(z, p_c) = \frac{\eta(\overline{p}^{1-\eta} - p_c^{1-\eta})z}{(\eta-1)(\overline{p}^{-\eta} - p_c^{-\eta})}.$$

Proof. Let $P(q,\overline{D})$ denote the inverse demand curve. Then, the welfare cost of z is

$$\begin{aligned}\text{WLC}(z, p_c) &= \left[\frac{z}{D(\overline{p},\overline{D}) - D(p_c,\overline{D})}\right]\int_{D(p_c,\overline{D})}^{D(\overline{p},\overline{D})} P(q,\overline{D})dq \\ &= \frac{z\eta(\overline{p}^{1-\eta} - p_c^{1-\eta})}{(\eta-1)(\overline{p}^{-\eta} - p_c^{-\eta})}.\end{aligned}$$

Note that $\overline{D}$ drops out of the welfare cost, which depends on the state only through the quantity z of rationing chosen at that state.

Appendix B

Extensions to the Model

Multiple Solar Observations per Hour

Most of our specifications, including our base specification, include solar data measured at the 15-minute level even though decision making occurs at the 1-hour level. In the interest of ease of exposition, the model described in Section III considered the case in which the decision making, solar output, and load all occur at the hourly level. We now consider the case in which there are $Y \geq 1$ solar observations per hour period.

Allowing for multiple solar observations per hour results in $\overline{S}$ being vector valued, $\overline{S} \equiv (\overline{S}^1, \ldots, \overline{S}^Y)$. Let $\overline{S}^{\text{mean}}$ denote the mean over the Y values, and $\overline{S}^{\min}$ the minimum over the Y values.

With this new model, (3), the transmission fixed costs will then include $\overline{S}^{\text{mean}}$ instead of $\overline{S}$. Equation (5), the outage event, substitutes $\overline{S}^{\min}$ for $\overline{S}$. Finally, for the system operators' second-stage maximization problem W in (6), the PC term becomes

$$\sum_{y=1}^{Y} PC(\overline{D}\overline{p}^{-\eta} - z - n^{SL}\overline{S}^y + LL(\overline{D}\overline{p}^{-\eta} - z - d^{SL}n^{SL}\overline{S}^y), \overrightarrow{x}(\overrightarrow{on})).$$

The model is then computable using this modified version of the operator's problem.

Real-Time Pricing

For this extension, we specify that an exogenous fraction γ of customers are on real-time pricing (RTP) contracts, with the remaining customers paying a fixed retail price. We assume that the system operator sets the real-time prices at the same time as scheduling generators, which is 1 day in advance. This RTP specification is similar to that of Borenstein and Holland (2005). In this extension, we eliminate demand-side management through curtailment contracts that are in the base model.

As before, $\overline{p}$ is the fixed retail price for customers not on RTP. Let $p^{\text{RTP}}(\overrightarrow{m}, \overrightarrow{w})$ be the real-time price, where we make explicit that this price is a function of maintenance status and the weather forecast. The demand for electricity is then

$$Q^D(p^{\text{RTP}}(\overrightarrow{m}, \overrightarrow{w}), \overline{p}, \overline{D}) = \begin{cases} \overline{D}(1-\gamma)\overline{p}^{-\eta} & p^{\text{RTP}}(\overrightarrow{m}, \overrightarrow{w}) > v \\ \overline{D}(\gamma p^{\text{RTP}}(\overrightarrow{m}, \overrightarrow{w})^{-\eta} + (1-\gamma)\overline{p}^{-\eta}) & p^{\text{RTP}}(\overrightarrow{m}, \overrightarrow{w}) \leq v. \end{cases} \quad \text{(B1)}$$

Our computation of the RTP solution solves for the optimal $p^{\text{RTP}}(\overrightarrow{m}, \overrightarrow{w})$ via a grid search. We let p^{RTP} be bounded between \$0 and \$5,000 per MWh.

Finally, note that there are many other potential demand-side management tools besides the two that we consider. For example, Borenstein (2012) explores the use of critical peak pricing (CPP) for residential customers. Customers on a CPP plan pay relatively low retail electricity prices except during a limited number of days of exceptionally high demand. These types of contracts could also be considered within our framework.

Imports and Exports

Finally, we add imports and exports to our model by introducing a net import supply function for the home (TEP, for our application) grid area. Denote the net import quantity as q^I; a positive value indicates imports into the home area and a negative value indicates exports from the home area. Correspondingly, denote the price of imports p^I. We assume that the system operator is faced with an expected net supply curve for imports of

$$q_t^I = \alpha_t^I + \beta^I \log p_t^I, \tag{B2}$$

where α_t^I, the import supply level, varies across hourly time periods t, and β^I is the net import supply semi-elasticity.

Our model with imports and exports is as follows. Net import decisions are made 1 day ahead, at the same time as scheduling generators. For each hour-long period, the operator observes $\overrightarrow{w}$, $\overrightarrow{m}$, and the net import supply curve for that time and then commits (except in the case of system outage) to a point on the net import supply curve.

The operator's objective function includes the cost (benefit) of imports (exports) but is otherwise the same as in the base model; she does not internalize the fact that if there is a system outage, she may not export the amount that she promised, which may cause system outages in other localities. In this extension, we do not allow demand-side management. The reason is that the system operator can obtain electricity at lower social cost by importing it than by curtailing demand. Our computation of the import/export solution solves for the optimal import quantity, as a function of $(t, \overrightarrow{w}, \overrightarrow{m})$, via a grid search.

We estimate the parameters of net import supply using the methods of Bushnell et al. (2008). Specifically, we parameterize α_t^I to include the cooling and heating needs of the surrounding states of California, Nevada, Utah, and New Mexico. For each of these states at each hour, we include for α_t^I the mean cooling and heating degree days and their squares.[39] We calculate the mean by averaging over all weather stations within a state. In addition to these 16 variables, we also include indicators for month, day of the week, and hour of the day in α_t^I. We also obtain p^I and q^I as described in Section IV.A.

As in Bushnell et al. (2008), we estimate (B2) with an instrumental variables regression and instrument for p^I with the local (TEP) load, as local load is correlated with p^I but not with the unobservable component of the operator's chosen import and export quantity. The unit of observation for our analysis is every hour during our sample period. We estimate $\beta^I = 8{,}862.2$ (with a standard error of 963.0). Our mean estimated α_t^I is $-30{,}616.4$. At the mean α_t^I, the system operator would pay \$32.70 per MWh to import 300 MW in an hour and would receive \$30.60 per MWh to export 300 MW in an hour.[40]

[39] Heating degree days is defined as 0 if the day's mean temperature is greater than 65, and it is equal to (65 − day's mean temperature) if the mean is less than 65. Cooling degree days is 0 if the day's mean temperature is less than 65 and as (day's mean temperature − 65) if the mean is greater than 65.

[40] Our numbers cannot directly be compared to those of Bushnell et al. (2008), since their equivalent of q^I included local production by a fringe.

Appendix C

Additional Figures and Tables

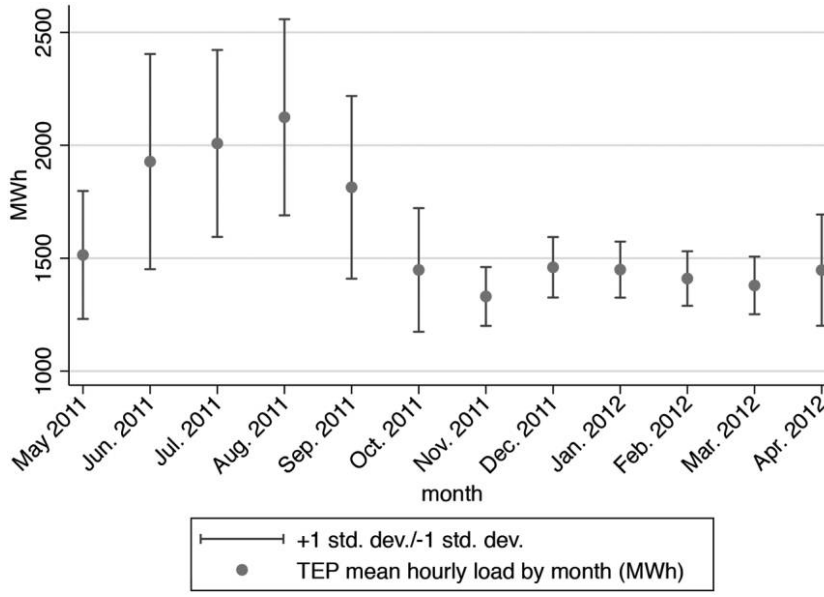

FIG. C1.—Summary statistics for TEP hourly load (MWh), May 2011–April 2012. Source: FERC Form 714. Color version available as an online enhancement.

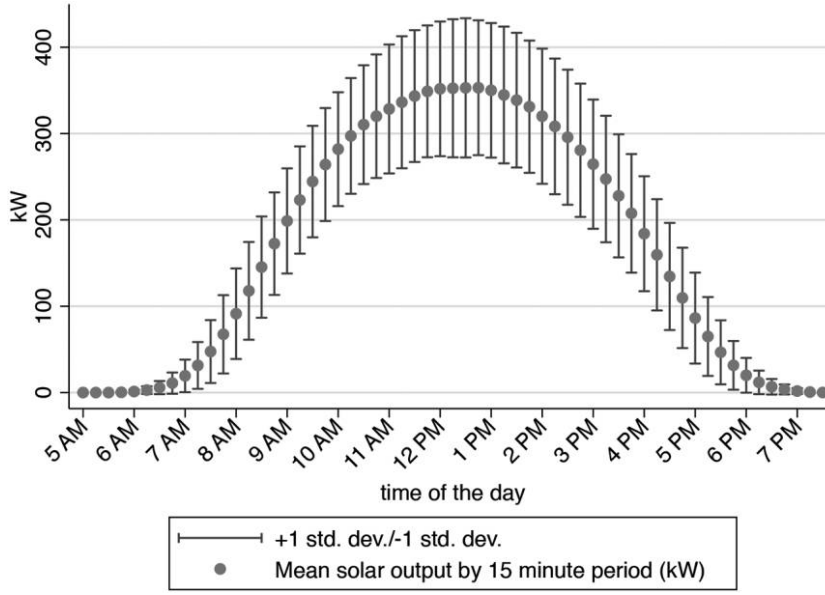

FIG. C2.—Summary statistics for Tucson solar output, 2011–12. Source: University of Arizona Photovoltaics Research Lab. Color version available as an online enhancement.

TABLE C1
SUMMARY STATISTICS FOR START-UP COSTS OF TEP GENERATORS, 2011–12

Unit Type	Number of Units	Additional Fuel Costs per Start-Up	Capital and Maintenance Costs per Start-Up	Total Costs per Start-Up
Solar PV	2	0	0	0
Coal (<300 MW)	3	20.30	132.70	152.90
Coal (>300 MW)	3	29.00	76.30	105.30
Natural gas combined cycle	1	1.00	56.30	57.30
Natural gas steam turbine	3	1.00	56.30	57.30
Natural gas turbine	6	1.90	87.00	88.90
Potential new natural gas combined cycle	. . .	1.00	56.30	57.30
Potential new natural gas turbine	. . .	1.90	87.00	88.90

SOURCE.—Kumar et al. (2012).
NOTE.—All costs are in $/MW.

TABLE C2
ESTIMATION OF DAYTIME LOAD AND SOLAR OUTPUT FORECASTS

	LOAD (MWh): COEFFICIENT ON SPLINE FOR			SOLAR OUTPUT (kWh): COEFFICIENT ON SPLINE FOR		
	1st Decile	5th Decile	10th Decile	1st Decile	5th Decile	10th Decile
Temperature	−25.7**	−2.3	39.0**	4.3**	1.5*	1.9**
	(1.4)	(1.3)	(1.0)	(.8)	(.7)	(.6)
Dew point	.6	7.7**	22.3**	−4.1**	−3.4**	−1.3
	(1.3)	(1.9)	(1.5)	(.7)	(1.0)	(.8)
Relative humidity	8.1*	−10.8**	−3.0**	10.2**	2.8**	1.6**
	(3.9)	(1.4)	(.6)	(2.1)	(.8)	(.3)
Wind	5.9*	−1.0	−2.1**	−3.7*	6.4**	1.2**
	(2.7)	(3.3)	(.5)	(1.5)	(1.8)	(.3)
Splines for cloud cover	2%–15%	38%–60%	78%–94%	2%–15%	38%–60%	78%–94%
Cloud cover	568**	296**	502**	−108**	−238**	−332**
	(52)	(51)	(102)	(28)	(27)	(55)
	LOAD (MWh): COEFFICIENT ON HOUR			SOLAR OUTPUT (kWh): COEFFICIENT ON HOUR		
	1	4	6	1	4	6
Hours since sunrise, a.m.	−146.2**	−55.5**	.7	43.3**	35.0**	36.4**
	(7.7)	(6.3)	(7.6)	(4.2)	(3.4)	(4.1)
Hours till sunset, p.m.	306.8	49.0**	8.6	63**	52.4**	35.1**
	(22.5)	(5.2)	(6.1)	(12.2)	(2.8)	(3.3)
Temperature × cloud	−7.5**	(.7)		1.5**	(.4)	
Relative humidity × cloud	−3.4**	(.7)		1.0**	(.4)	
Wind × cloud	−1.6*	(.7)		−4.6**	(.4)	
Dew × cloud	5.8**	(.8)		−.2	(.5)	
6 a.m. dummy	132**	(8.3)		−5.3	(4.5)	
12 noon dummy	667**	(31.1)		124**	(16.8)	
6 p.m. dummy	118**	(20.3)		−93**	(11.0)	
R^2	.959			.878		
MAPE	3.4%					
rRMSE				.234		
Correlation of residuals				.093**		

NOTE.—The model is estimated with an SUR specification. The unit of observation is 15-minute intervals in May 2011–April 2012. Standard errors are clustered at the hour level. The number of observations is 17,825. We include as regressors day-of-week and month-of-year indicators and full sets of spline coefficients. MAPE is the mean absolute percentage error; rRMSE is the relative root mean squared error.

* Statistically significant at the 5 percent level.

** Statistically significant at the 1 percent level.

TABLE C3
Estimation of Nighttime Load Forecast

	Load (MWh): Coefficient on Spline for		
	1st Decile	5th Decile	10th Decile
Temperature	−22.0**	2.2	36.7**
	(2.8)	(2.5)	(5.3)
Dew point	3.9	8.2*	12.7**
	(3.0)	(3.2)	(3.3)
Relative humidity	−.3	−6.3*	−3.1**
	(9.1)	(3.0)	(1.0)
Wind	−5.0	−3.2	−5.4**
	(4.1)	(4.0)	(1.2)
Splines for cloud cover	2%–15%	38%–60%	78%–94%
Cloud cover	257**	83	31
	(74)	(69)	(130)
Temperature × cloud cover	−5.5**	(1.2)	
Relative humidity × cloud cover	−1.6*	(.8)	
Wind × cloud cover	4.1**	(1.4)	
Dew point × cloud cover	5.1**	(1.5)	
9 p.m. dummy	263**	(5.5)	
3 a.m. dummy	−67**	(4.1)	
R^2	.945		
MAPE	3.2%		

Note.—The model is estimated with ordinary least squares. The unit of observation is 15-minute intervals in May 2011–April 2012. Standard errors are clustered at the hour level. The number of observations is 17,311. We include as regressors day-of-week and month-of-year indicators and full sets of spline coefficients. MAPE is the mean absolute percentage error.

* Statistically significant at the 5 percent level.

** Statistically significant at the 1 percent level.

TABLE C4
Detailed Results for Base Specification in Table 5

	Fraction of Generation from Solar			
	0%	10%	15%	20%
Solar PV capacity (MW)	0	941	1,411	1,881
Solar production (1,000 MWh/year)	0	1,694	2,541	3,387
Load (1,000 MWh/year)	16,937	16,937	16,937	16,937
New 191 MW natural gas generators (N)	10	8	8	7
Forgone new gas generators (N)	0	2	2	3
Scheduled nonsolar production + reserves (1,000 MWh/year)	24,021	22,466	21,852	21,216
Realized nonsolar production + reserves (1,000 MWh/year)	24,003	22,449	21,835	21,199
Reserves as % of energy consumed	30.5	32.1	33.6	35.2
Average system outage probability	4.76e−5	5.82e−5	5.81e−5	8.4e−5
Curtailment price p_c ($/MWh)	661	469	431	804
Total curtailment (as % of total load)	.11	.19	.14	.24
Probability of some curtailment July 12 noon	.033	.032	7.8e−5	2.6e−7
Probability of some curtailment July 6 p.m.	.097	.37	.33	.58

TABLE C4 (*Continued*)

	Fraction of Generation from Solar			
	0%	10%	15%	20%
Production costs	437.20	380.00	355.20	332.20
Reserve costs	78.10	81.50	82.80	84.80
Gas generator investment costs	2,090	1,672	1,672	1,463
Solar capacity investment costs	0	4,148	6,221	8,295
Transmission FC	331.4	319.4	317.4	316.2
Transmission line losses (1,000 MWh/year)	1,480	1,378	1,335	1,287
Probability of natural gas generator scheduled	.97	.97	.95	.90
Loss in surplus relative to baseline (million $/year)	. . .	214.50	339.70	468.90
Loss in surplus per unit solar production ($/MWh)	. . .	126.70	133.70	138.40
Loss in $ surplus per ton CO_2 reduced	. . .	293.10	283.50	279.10
NO_x emissions (1,000 metric tons/year)	12.8	12.6	12.2	11.8
SO_2 emissions (1,000 metric tons/year)	6.3	6.3	6.1	6.0
CO_2 emissions (million metric tons/year)	15.1	14.4	13.9	13.4

Note.—Cost variables are measured in millions of dollars per year.

TABLE C5
The Social Costs of Large-Scale Solar Including Start-Up Costs

	Fraction of Generation from Solar			
	0%	10%	15%	20%
Start-up costs	20.90	24.00	29.80	38.70
Loss in surplus per unit solar production ($/MWh)	. . .	128.50	137.20	143.70

Note.—Cost variables are measured in millions of dollars per year.

References

Baker, E., M. Fowlie, D. Lemoine, and S. Reynolds. 2013. "The Economics of Solar Electricity." *Ann. Revs. Resource Econ.* 5:387–426.

Baldick, R., S. Kolos, and S. Tompaidis. 2006. "Interruptible Electricity Contracts from an Electricity Retailer's Point of View: Valuation and Optimal Interruption." *Operations Res.* 54:627–42.

Barbose, G., N. Darghouth, S. Weaver, and R. Wiser. 2013. "Tracking the Sun VI: An Historical Summary of the Installed Price of Photovoltaics in the United States from 1998 to 2012." Technical report, Ernest Orlando Lawrence Berkeley Nat. Lab., Berkeley, CA.

Baughman, M., and D. Bottaro. 1976. "Electric Power Transmission and Distribution Systems: Costs and Their Allocation." *IEEE Trans. Power Apparatus and Systems* 95 (3): 782–90.

Bohn, R., M. Caramanis, and F. Schweppe. 1984. "Optimal Pricing in Electrical Networks over Space and Time." *RAND J. Econ.* 15:469–93.

Borenstein, S. 2008. "The Market Value and Cost of Solar Photovoltaic Electricity Production." Working Paper no. 176, Center Study Energy Markets, Univ. California, Berkeley.

———. 2012. "Effective and Equitable Adoption of Opt-In Residential Dynamic Electricity Pricing." Working Paper no. 229, Energy Inst., Haas School, Univ. California, Berkeley.
Borenstein, S., J. Bushnell, and F. Wolak. 2002. "Measuring Market Inefficiencies in California's Restructured Wholesale Electricity Market." *A.E.R.* 92:1376–1405.
Borenstein, S., and S. Holland. 2005. "On the Efficiency of Competitive Electricity Markets with Time-Invariant Retail Prices." *RAND J. Econ.* 36:469–93.
Bouffard, F., F. Galiana, and A. Conejo. 2005. "Market-Clearing with Stochastic Security—Part I: Formulation." *IEEE Trans. Power Systems* 20 (4):1818–26.
Bushnell, J., E. Mansur, and C. Saravia. 2008. "Vertical Arrangements, Market Structure, and Competition: An Analysis of Restructured U.S. Electricity Markets." *A.E.R.* 98:237–66.
Campbell, A. 2011. "Government Support for Intermittent Renewable Generation Technologies." Working paper, School Management, Yale Univ.
Cramton, P., and J. Lien. 2000. "Value of Lost Load." Working paper, Univ. Maryland.
Cramton, P., A. Ockenfels, and S. Stoft. 2013. "Capacity Market Fundamentals." *Econ. Energy and Environmental Policy* 2 (2).
Cullen, J. 2010a. "Dynamic Response to Environmental Regulation in Electricity Markets." Working paper, Harvard Univ.
———. 2010b. "Measuring the Environmental Benefits of Wind Generated Electricity." Working paper, Harvard Univ.
Cullen, J., and S. Reynolds. 2016. "The Long Run Impact of Environmental Policies on Wholesale Electricity Markets: A Dynamic Competitive Analysis." Manuscript, Univ. Arizona.
Denholm, P., and R. Margolis. 2007. "Evaluating the Limits of Solar Photovoltaics (PV) in Traditional Electric Power Systems." *Energy Policy* 35:2852–61.
EIA (Energy Information Administration). 2010. "Electric Power Monthly." http://www.eia.gov/electricity/monthly/backissues/html.
———. 2011. "Continuous Emissions Monitoring System." http://ampd.epa.gov/ampd.
———. 2012. "Renewable Capacity in the Annual Energy Outlook 2012." http://www.eia.gov/forecasts/archive/aeo12/.
———. 2013. "Updated Capital Cost Estimates for Utility Scale Electricity Generating Plants." http://eia.gov/forecasts/capitalcost/pdf/updated_capcost.pdf.
———. 2014a. "Electric Power Monthly." http://www.eia.gov/electricity/monthly/current_year/january2014.pdf.
———. 2014b. "Levelized Cost of New Generation Resources in the Annual Energy Outlook 2014." http://www.eia.gov/forecasts/aeo/pdf/electricity_generation.pdf.
Ela, E., M. Milligan, and B. Kirby. 2011. "Operating Reserves and Variable Generation." Technical Report TP-5500-51978, National Renewable Energy Lab., Golden, CO.
EPA (Environmental Protection Agency). 2011. "NOx Budget Trading Program, Compliance and Environmental Results, 2007." http://www.epa.gov/sites/production/files/2015-08/documents/2007-nbp-report.pdf.
———. 2015. "The Social Cost of Carbon." http://www.epa.gov/climatechange/EPAactivities/economics/scc.html.
ERCOT (Electric Reliability Council of Texas). 2011. "Day-Ahead Ancillary Services Market Clearing Prices for Capacity." http://www.ercot.com/mktinfo/prices/mcpc.

Espey, J., and M. Espey. 2004. "Turning On the Lights: A Meta-Analysis of Residential Electricity Demand Elasticities." *J. Agricultural and Appl. Econ.* 36:65–81.
Fabbri, A., T. Romn, J. Abbad, and V. Quezada. 2005. "Assessment of the Cost Associated with Wind Generation Prediction Errors in a Liberalized Electricity Market." *IEEE Trans. Power Systems* 20:1440–46.
Fay, D., and J. Ringwood. 2010. "On the Influence of Weather Forecast Error in Short-Term Load Forecasting Models." *IEEE Trans. Power Systems* 25 (3): 1751–58.
FERC (Federal Energy Regulatory Commission). 2012. "Assessment of Demand Response and Advanced Metering." Technical report, Fed. Energy Regulatory Comm., Washington, DC.
GE Energy. 2008. "Analysis of Wind Generation Impact on ERCOT Ancillary Services Requirements." Report, Electric Reliability Council of Texas, Austin.
Hydro One. 2012. "Business Load Forecast and Methodology." http://www.hydroone.com/RegulatoryAffairs/Documents/EB-2012-0031/Exhibit%20A/A-15-02.pdf.
Independent Electricity System Operator. 2012. "Joint Optimization of Energy and Operating Reserve." http://www.ieso.ca/imoweb/pubs/training/QT20_JointOptimization.pdf.
Joskow, P. 2011. "Comparing the Costs of Intermittent and Dispatchable Electricity Generating Technologies." *A.E.R. Papers and Proc.* 101 (3): 238–41.
Joskow, P., and J. Tirole. 2007. "Reliability and Competitive Electricity Markets." *RAND J. Econ.* 38:60–84.
Krishna, V. 2010. *Auction Theory*. 2nd ed. Amsterdam: Elsevier.
Kumar, N., P. Besuner, S. Lefton, and D. Agan. 2012. "Power Plant Cycling Costs." http://www.nrel.gov/docs/fy12osti/55433.pdf.
Lamont, A. 2008. "Assessing the Long-Term System Value of Intermittent Electric Generation Technologies." *Energy Econ.* 30:1208–31.
Larson, V. 2013. "Forecasting Solar Irradiance with Numerical Weather Prediction Models." In *Solar Energy Forecasting and Resource Assessment*, edited by J. Kleissl, 299–318. New York: Academic Press.
Lueken, C., G. Cohen, and J. Apt. 2012. "Costs of Solar and Wind Power Variability for Reducing CO_2 Emissions." *Environmental Sci. and Tech.* 46 (17): 9761–67.
Madaeni, S., and R. Sioshansi. 2013. "The Impacts of Stochastic Programming and Demand Response on Wind Integration." *Energy Systems* 4:109–24.
Milligan, M., et al. 2011. "Integration of Variable Generation, Cost-Causation, and Integration Costs." *Electricity J.* 24 (9): 51–63.
Mills, A., A. Botterud, J. Wu, Z. Zhou, B. Hodge, and M. Heaney. 2013. "Integrating Solar PV in Utility System Operations." Technical report. Working paper no. ANL/DIS-13/18, Argonne Nat. Lab., Lemont, IL.
Mills, A., and R. Wiser. 2010. "Implications of Wide-Area Geographic Diversity for Short-Term Variability of Solar Power." Technical report. Working paper no. LBNL-3884E, Ernest Orlando Lawrence Berkeley Nat. Lab., Berkeley, CA.
———. 2012a. "Changes in the Economic Value of Variable Generation at High Penetration Levels: A Pilot Case Study of California." Technical report. Working paper no. LBNL-5445E, Ernest Orlando Lawrence Berkeley Nat. Lab., Berkeley, CA.
———. 2012b. "An Evaluation of Solar Valuation Methods Used in Utility Planning and Procurement Processes." Technical report. Working paper no. LBNL-5933E, Ernest Orlando Lawrence Berkeley Nat. Lab., Berkeley, CA.
Muller, N., and R. Mendelsohn. 2009. "Efficient Pollution Regulation: Getting the Prices Right." *A.E.R.* 99 (5): 1714–39.

National Renewable Energy Laboratory. 2011. "Solar Photovoltaic Technology." http://www.nrel.gov/learning/re_photovoltaics.html.

NERC (North American Electric Reliability Corporation). 2015. "Contingency Reserve." WECC standard BAL-002-WECC-2. http://www.nerc.com/files/BAL-002-WECC-2.pdf.

Reguant, M. 2014. "Complementary Bidding Mechanisms and Startup Costs in Electricity Markets." *Rev. Econ. Studies* 81 (4): 1708–42.

Roca, M. 2013. "Annual Solar Installs to Beat Wind for First Time." *Bloomberg New Energy Finance*, September 26.

Schmalensee, R., and R. Stavins. 2013. "The SO_2 Allowance Trading System: The Ironic History of a Grand Policy Experiment." *J. Econ. Perspectives* 27 (1): 103–22.

Sigrin, B., P. Sullivan, E. Ibanez, and R. Margolis. 2014. "Representation of the Solar Capacity Value in the ReEDS Capacity Expansion Model." http://www.nrel.gov/docs/fy14osti/62015.pdf.

Skea, J., D. Anderson, T. Green, R. Gross, P. Heptonstall, and M. Leach. 2008. "Intermittent Renewable Generation and the Cost of Maintaining Power System Reliability." *IET General Transmission Distribution* 2 (1): 82–89.

TEP (Tucson Electric Power). 2012. "Tucson Electric Power 2011 Renewable Energy Standard and Tariff Compliance Report." http://www.azcc.gov/Divisions/Utilities/2011%20TEP%20REST.pdf.

Tuohy, A., P. Meibom, E. Denny, and M. O'Malley. 2009. "Unit Commitment for Systems with Significant Wind Penetration." *IEEE Trans. Power Systems* 24:592–601.

UniSource. 2012. "UniSource Energy Corp 10-K Report for 2011." http://http://www.sec.gov/Archives/edgar/data/100122/000119312512082165/d285669d10k.htm.

Weron, R., and A. Misiorek. 2004. "Modeling and Forecasting Electricity Loads: A Comparison." In *European Electricity Market EEM-04 Conference Proceedings*. University Park, PA: Citeseer.

Wolfram, C. 1999. "Measuring Duopoly Power in the British Electricity Spot Market." *A.E.R.* 89:805–26.

———. 2005. "The Efficiency of Electricity Generation in the United States after Restructuring." In *Electricity Deregulation: Choices and Challenges*, edited by J. Griffin and S. Puller. Chicago: Univ. Chicago Press.